UNIVERSITÉ DU QUÉBEC À MONTRÉAL

VALIDATION D'UNE NOUVELLE APPROCHE POUR ESTIMER L'ÉVAPORATION DE RÉSERVOIRS ET ANALYSE GLOBALE DE L'INFLUENCE DE LEURS CARACTÉRISTIQUES SUR LEUR TAUX D'ÉVAPORATION ANNUEL

MÉMOIRE

PRÉSENTÉ

COMME EXIGENCE PARTIELLE

DE LA MAITRISE EN BIOLOGIE

PAR

GABRIEL BASTIEN-BEAUDET

JUILLET 2023

REMERCIEMENTS

First, I am grateful to my supervisor, Yves Prairie, for his guidance, scientific support and for always being readily available. I am also thankful to you for your confidence in supporting the project I initially brought up to you, even though I ended up working on something completely different. Thank you for sparking my interest in a subject I would have never thought of by myself.

I am thankful to the funding agencies that supported this project. Thanks to Hydro-Québec, MITACS and the UNESCO chair in global environmental change.

I would like to thank Daniel Nadeau and Dominic Serça for sharing their data and making my master's possible. I also thank Copernicus Climate Change Services, the Swiss Federal Institute of Aquatic Science and Technology and Global HydroLAB for making their data publicly available.

For their confidence in hiring me as an undergrad for jobs that sparked my interest in limnology, I am thankful to Alice Parkes, Serge Paquet, Marie-Pierre Varin, Yannick Huot and Paul del Giorgio. For fieldwork fun that kept me going through my undergrad studies, I thank Jean-Christophe Sicotte-Brisson, Felipe Rust, Maximilian Lau, Masumi Stadler, Christoforos Pappas, Daniel Kneeshaw's lab team, Karelle Desrosiers and the L-Care team. I'd also like to thank Jihyeon Kim and Sara Mercier-Blais for their help, tips, and guidance throughout my master's.

I would like to mention my appreciation to Gareth R. Hopkins, for understandably teaching statistics (finally), for sharing its open science philosophy and for changing my view on science communication, or even on science in general.

My deepest gratitude goes to my girlfriend, for supporting me through the ups and downs of graduate studies, always being excited by my work, believing in me much more than I do and for being the best and strongest mother (and girlfriend) I could ask for.

DÉDICACES

Try harder. Make it count.

- CN

TABLE DES MATIÈRES

LISTE DES FIGURES

LISTE DES TABLEAUX

LISTE DES ABRÉVIATIONS, DES SIGLES ET DES ACRONYMES

Abbreviation	Description	Units
a_{seiche}	Fraction of seiche energy to total wind energy	Dimensionless
A_n	Advected energy	MJ m^{-1}
A_s	Surface area	km^2
A_z	Area at depth "z"	km^2
BREB	Bowen Ratio Energy Budget	-
CCCS	Copernicus Climate Change Services	-
CDOM	Colored Dissolved Organic Matter	-
c_p	Specific heat of air	MJ Kg^{-1} $°C^{-1}$
c_w	Specifi heat of water	MJ Kg^{-1} $°C^{-1}$
d_t/d_z	Temperature gradiant between t_w and sediments	°C
E	Evaporation	mm day^{-1}
e^*_s	Saturation vapor pressure at the water surface	Pa
e_a	Vapor pressure of air	Pa
Eawag	Swiss Federal Institute of Aquatic Science and Technology	-
ECMWF	European Centre for Medium-range Weather Forecast	-
$f_{(u)}$	Wind function	-
G_n	Sediment heat conduction	MJ m^{-2}
GAM	Generalized additive models	-
H	Sensible heat	MJ m^{-2}
K_c	Bulk exchange coefficient	W m^{-2} $°K^{-1}$
K_d	Light extinction coefficient	m^{-1}
K_{sed}	Sediment heat transfer conductivity	W m^{-1} $°C^{-1}$
L	Latent heat	MJ m^{-2}
MAE	Mean Absolute Error	Data dependant
MBE	Mean Bias Error	Data dependant
N	Heat storage	MJ m^{-2}
NT2	Nam Theun 2	-
p_w	Density of water	Kg m^{-3}
q_a	Specific humidity of air	g Kg^{-1}
q_s	Specific humidity at the water surface	g Kg^{-1}
R	Correlation coefficient	Dimensionless
R^2	Coefficient of determination	Dimensionless
R_{il}	Incoming longwave radiations	MJ m^{-2} or W^{-2}
RMSE	Root Mean Square Error	Data dependant
R_n	Net radiations at the water surface	MJ m^{-2} or W^{-2}
R_{nl}	Net longwave radiations	MJ m^{-2} or W^{-2}
R_{ns}	Net shortwave radiations	MJ m^{-2} or W^{-2}
RO2	La Romaine 2	-
R_{ol}	Outgoing longwave radiations	MJ m^{-2} or W^{-2}
R_{os}	Outgoing shortwave radiations	MJ m^{-2} or W^{-2}
R_s or R_{is}	Incoming shortwave radiations	MJ m^{-2} or W^{-2}
SML	Surface mixed layer	-
T_a	Air temperature	°C
T_{dew}	Dewpoint temperature	°C
T_s	Surface water temperature	°C
T_w	Water temperature over the sediments	°C
T_{yr}	Mean annual whole lake temperature	°C
U	Wind speed	m s^{-1}
VPD	Vapor pressure deficit	kPa
Z	Depth	m
z_{max}	Maximum depth	m
z_{mean}	Average depth	m
Z_{sed}	Depth over which sediment temperature would increase from T_{yr} to T_w	m
Z_{therm}	Thermocline depth	m

LISTE DES SYMBOLES ET DES UNITÉS

Symbol or Unit	Description
$\emptyset$	Atmospheric pressure (kPa)
α	Albedo (dimensionless)
β	Bowen ratio (dimensionless)
ΔT_z	Change in mean lake temperature at depth "z" over time "t" (°C)
Δ_z	Discretized water body layer thickness (m)
ε	Emissivity of water (dimensionless)
ε_m	Ratio of molecular weight of water to that of dry air (dimensionless)
γ	Psychrometric constant ($c_p \emptyset / \varepsilon_m \lambda$)
λ	Latent heat of evaporation (MJ Kg^{-1})
σ	Stefan-Boltzmann constant (MJ m^{-2} $°K^{-1}$)
°C	Degree Kelvin
°K	Degree Kelvin
g	Gram
Hz	Hertz
J	Joule
Kg	Kilogram
Km	Kilometer
kPa	Kilopascal
MJ	Megajoule
m	Meter
mm	Millimeter
min	Minute
Pa	Pascal
%	Percent
s	Second
W	Watt

RÉSUMÉ

L'eau est une ressource de plus en plus rare que nous tenons malgré tout pour acquise. Les pertes d'eau peuvent être attribuées à de nombreux phénomènes tels que la surpopulation, la surconsommation et les changements climatiques, qui entraînent à leur tour l'épuisement des nappes phréatiques, des sécheresses fréquentes et intenses, et la contamination de l'eau. Une perte présentement négligée est l'évaporation des réservoirs d'eau douce. Ces pertes représentent une quantité d'eau importante, estimée à 11 % de l'empreinte eau de l'humanité selon Hoekstra et Mekonnen (2011). Les défis associés à la mesure et l'estimation de l'évaporation ralentissent notre compréhension de ce phénomène. Dans cette étude, nous avons développé une méthode qui adresse ces défis, applicable à la majorité des étendus d'eau. Pour ce faire, nous avons combiné réanalyse climatique et modélisation physique de lac, puis combiner un budget énergétique et une équation aérodynamique pour estimer l'évaporation. Les deux équations ont d'abord été validées avec des données météorologiques *in situ*, contre des données de covariance d'Eddy issues deux réservoirs avec des morphologies différentes et dans des climats différents. Les deux équations ont bien performé, avec des RMSE variant entre 0,85 et 1,75 mm jour^{-1} et des coefficients R de 0,75 à 0,86. L'approche multi-modèle consistant en la moyenne des deux équations a amélioré considérablement la performance de l'approche sur les deux réservoirs. Lorsqu'elle est utilisée avec des données météorologiques de réanalyse climatique, la performance de l'approche multi-modèle a diminué, avec des RMSE de 1,05 et 0,98 mm jour^{-1}, et des coefficients R de 0,86 et 0,84. Avec cette nouvelle méthode, nous avons étendu notre analyse à l'échelle mondiale. Nous avons cherché à identifier les relations avec la morphologie et les propriétés physiques des réservoirs afin d'améliorer la gestion des ressources et de contribuer à l'évaluation des risques liés à la pénurie d'eau. Pour ce faire, nous avons modélisé l'évaporation annuelle de 187 réservoirs dispersés dans le monde entier, dans des conditions climatiques diverses et avec des caractéristiques variées. Les taux d'évaporation des réservoirs variaient entre 152 et 1792 millimètres par année avec une moyenne de 927, et représentaient en moyenne 6.4% de leur débit annuel moyen. Aucune relation n'a été trouvée entre la morphologie et l'évaporation annuelle, mais un modèle additif généralisé reliant l'évaporation à la profondeur de la thermocline et la durée de la stratification a expliqué 77% de la déviance du modèle, avec un R^2 de 0,76. L'évaporation annuelle était moindre à des thermoclines peu profondes, à partir de 2 mètres. L'évaporation augmentait jusqu'à 6 mètres, où elle était à son maximum et constante pour les thermoclines plus profondes. La réduction des pertes de chaleur dues à la diminution de la différence de température entre la surface de l'eau et l'atmosphère ainsi que le refroidissement de l'eau de surface induite par le vent et l'évaporation ont été

suggérées pour expliquer cette relation. L'évaporation annuelle était la plus élevée avec une courte durée de stratification, de 1 à 160 jours, et se stabilisait à son niveau le plus bas pour des durées plus longues. La stabilité réduite et le faible gradient de densité dans la colonne d'eau causés par des taux d'évaporation élevés pourrait expliquer cette relation. Dans l'ensemble, nous concluons d'abord que la méthodologie proposée est une contribution importante, car elle pourrait être utilisée pour estimer l'évaporation de réservoirs difficiles d'accès, ne disposant pas de stations météorologiques ou pour prédire l'évaporation de futurs réservoirs. De plus, nous considérons que la profondeur de la thermocline et la durée de la stratification constituent une bonne plateforme pour prédire l'évaporation des réservoirs. Elles sont plus faciles à mesurer ou à prédire que l'évaporation réelle, offrant ainsi une alternative à une logistique complexe et chronophage. Nous pensons que nos résultats peuvent être utilisés pour améliorer la gestion des ressources hydriques et fournir des indications pour la conception de réservoirs à pertes d'eau et empreinte eau réduite.

Mots clés: évaporation, limnologie, hydrologie, lacs, réservoirs, pénurie de l'eau, empreinte eau.

ABSTRACT

Water is an increasingly scarce resource that we still take for granted. Water losses can be attributed to several phenomena like overpopulation, overconsumption, and climate changes which in turn cause groundwater depletion, droughts, and water contamination. An overlooked water loss is evaporation from freshwater reservoirs. These losses can represent a substantial amount of water, estimated at 11% of humanity's water footprint according to Hoekstra and Mekonnen (2011). Challenges in the measurement and estimation of evaporation are however slowing down our comprehension of this phenomenon. In this study, we developed a method that addresses these challenges, applicable for most water bodies around the globe, with limited or absent data availability. We did so by combining climate reanalysis with physical lake modelling and computing an energy budget and an aerodynamic equation for estimating evaporation. Both equations were validated when driven by *in situ* meteorological data, against eddy covariance datasets, over two different reservoirs with contrasting morphologies and in different climates. Both equations performed well, with RMSEs varying between 0.85 and 1.75 mm day^{-1} and R coefficients, from 0.75 to 0.86. The multi-model approach consisting of averaging the outputs of both equations improved results at both reservoirs significantly. When driven by climate reanalysis inputs, the performance of the multi-model approach decreased, with RMSEs of 1.05 and 0.98 mm day^{-1}, and R coefficients of 0.86 and 0.84. With this new method, we upscaled our analysis to the global scale. We aimed to identify relationships with the reservoir's morphology and physical properties to improve resource management and contribute to risk assessment related to water scarcity. We did so by modelling annual evaporation from 187 reservoirs dispersed around the globe, in diverse climatic conditions and with various characteristics. Evaporation rates from reservoirs varied between 152 and 1972 millimeters per year witn a mean of 927, and represented on average 6.4% of their mean annual inflow. No relations were found between morphology and annual evaporation, but a generalized additive model relating evaporation with thermocline depth and duration of stratification explained 77% of the model's deviance, with an R^2 of 0.76. Annual evaporation was lowest with lower thermoclines, starting at 2 meters. Evaporation then followed a linear relationship up to 6 meters, where it was at its highest and constant for deeper thermoclines. Reduced heat losses from the lowered temperature differences between the water surface and the atmosphere and surface cooling induced by wind and evaporative were suggested as explanations for this relationship. Annual evaporation was highest with a short duration of stratification from 1 day up to 160 days and stabilized at its lowest for longer durations. We believe reduced stability and density gradient caused by high evaporation rates can explain this relation. Overall, we conclude first

that our proposed methodology is an important contribution, as it could be applied to estimate the evaporation of reservoirs that are difficult to access, don't have meteorological stations or to predict evaporation of future impoundments. Moreover, we think that thermocline depth and duration of stratification constitute a good proxy for predicting evaporation from reservoirs. It is easier to measure or predict than actual evaporation, offering an alternative to complex, time-consuming logistics. We believe that our results can be used to improve water resource management and provide indications on ways to design reservoirs with reduced evaporative water losses and water footprints.

Keywords: evaporation, limnology, hydrology, lakes, reservoirs, water crisis, water footprint.

INTRODUCTION

Un accroissement démographique persistant se traduit inévitablement en un accroissement de la demande de diverses ressources. En revanche, une demande croissante ne garantit pas une offre croissante et certaines ressources prises pour acquises deviennent de plus en plus limitées. L'eau potable en est un exemple probant. En effet, on estime à 4 milliards le nombre d'individus ressentant les effets d'une pénurie d'eau sévère sur une période d'au moins un mois par année et à 500 millions, ceux qui en ressente l'effet à l'année longue (Mekonnen et Hoekstra, 2016). C'est pour cette raison que le concept « d'empreinte eau » gagne en popularité, exprimant la quantité d'eau douce consommée ou polluée par un produit, un procédé, une entreprise ou quelconque entité pour sa production et/ou son opération. Hoekstra et Mekonnen (2011) ont estimés l'empreinte eau de l'humanité à 9087 milliards de mètres cube d'eau par année, de 1996 à 2005. 11% de cette empreinte a été attribué à l'évaporation de surfaces d'eau libre.

Les réservoirs d'eau douce ont donc eux-mêmes une empreinte eau due à leur perte par évaporation. Ces pertes peuvent représenter une quantité d'eau douce substantielle. Par exemple, Zhao et Gao (2019) ont estimés la quantité d'eau perdue annuellement par évaporation de 721 réservoirs aux États-Unis à 33,73 milliards de mètres cube, de 1985 à 2014, une quantité représentant 93% de leur réserve d'eau annuel publique en 2010. De plus, l'Australie perd 40% de sa capacité totale de stockage d'eau annuelle par évaporation (Craig et al., 2005) et le Texas en perd l'équivalent de 126% de l'utilisation municipal d'eau uniquement par évaporation de ses réservoirs (Wurbs et Alaya, 2014). L'eau est effectivement une ressource renouvelable, c'est-à-dire qu'elle ne disparait pas éternellement lorsqu'elle s'évapore puisqu'elle revient sous forme de précipitations. Cependant, celles-ci ne reviennent pas nécessairement au bon endroit ni au bon moment pour compenser les pertes (Oki et Kanae, 2006). Ceci est d'autant plus important si les prédictions concernant l'augmentation de la fréquence d'évènement météorologique et climatique extrême s'avèrent véridiques (Huntington, 2006). La pénurie d'eau représente un problème important dans plusieurs pays, incluant certaines puissances mondiales telle que les États-Unis. De plus, les effets d'un épuisement local d'eau se fait sentir à plus grande échelle, puisque différents pays dépendent des autres pour la production de ressources au moyen de l'agriculture, pour la production d'énergie, ou simplement pour l'accès à l'eau potable (Oki et Kanae, 2006).

Conséquemment, l'habileté d'estimer l'évaporation d'étendue d'eau libre et d'interpréter adéquatement ses tendances historiques est d'une importance capitale, puisqu'elle nous permet de prédire les tendances futures qui affecteront potentiellement l'accès à l'eau douce et potable à l'échelle mondiale. Plus important encore, cette habileté peut être utilisée pour le développement d'outils de gestion de ressources hydriques ainsi que l'évaluation et la gestion de risques associés à la pénurie de l'eau. Finalement, elle peut être utilisée pour l'identification des effets de la morphologie et les caractéristiques physiques des réservoirs sur leur taux d'évaporation, ce qui nous permettrait de concevoir des réservoirs à empreinte eau réduite en atténuant leur perte par évaporation.

Les mesures directes et les méthodes d'estimations

L'évaporation d'une étendue d'eau se rapporte à la chaleur latente, une forme d'énergie qui ne se reflète pas dans les changements de température de l'eau. Ceci rend sa mesure directe complexe au niveau logistique, dispendieuse, et nécessite beaucoup de temps ainsi que de préparation. Les campagnes d'échantillonnage qui y sont dédiées sont donc généralement courte ou bien ne couvre qu'une petite partie de la zone à l'étude (Burba et Anderson, 2010). Les campagnes les plus longues connues furent d'une durée de 4 ans avec multiples intervalles manquants (Du et al., 2018) ou de 4 saisons estivales (aucune mesure lors de la présence de glaçe) (Nordbo et al., 2011). Il en découle des difficultés ainsi que de l'imprécision lors de l'interprétation de tendances à long terme ainsi qu'à grande échelle spatiale. Cette problématique a induit le développement de multiples méthodes d'estimation de l'évaporation, chacune avec leur propre exigences, conditions d'application, paramètres requis et limitations (Finch et Calver, 2008). La plupart de ces méthodes sont efficaces pour un système ou une configuration spécifique (climat, morphologie, type d'étendue d'eau, etc.), mais un consensus n'a toujours pas été atteint quant à une méthode standardisée qui pourrait être utilisée efficacement sur n'importe quel lac ou réservoir, dans n'importe quelle configuration (McMahon et al., 2013). Plusieurs méthodes ont aussi été développée pour pallier des données historiques limitées ou absentes. Par conséquent, la littérature se concentre surtout sur la validation et la performance de différents modèles et méthodes sur des lacs individuels plutôt que d'analyser des tendances spatio-temporelles. Les quelques études qui s'intéressent à ces tendances utilisent des méthodes d'estimation différentes produisant parfois des résultats contradictoires (McMahon et al., 2013 et références y figurant). L'emphase sur des modèles reposant sur des relations ou des conditions d'application sans fondement ou sur des coefficients nécessitant une calibration a aussi été soulignée, ce qui semble provenir de connaissances restreintes de certains concepts hydrologiques

(Morton, 1994). Pour ces raisons, l'interprétation des tendances d'évaporation temporelles et spatiales sont difficile à identifier, valider et comparer entre elles.

L'accumulation de données historiques et le développement d'outils modernes tel que la réanalyse météorologique constituent une opportunité pour estimer les taux d'évaporation du passé. En revanche, ce type d'analyse apporte plus de questions que de réponses au sein de la communauté scientifique puisque les tendances observées (ou leur absence) et leur interprétation diffère d'une étude à une autre (Brutsaert et Parlange, 1998; Huntington, 2006; Koutsoyiannis, 2020; Roderick and Farquhar, 2002). Ceci semble provenir d'une interaction complexe entre les différentes variables utilisées dans les modèles, le niveau d'incertitude de ces derniers et un désaccord par rapport à un niveau de sensibilité acceptable. Des tendances différentes apparaissent lors de l'observation de taux d'évaporation à différentes échelles temporelles, suggérant des tendances s'inversant au fil du temps (Lenters et al., 2005; Wang et al., 2018). Distinguer les variations naturelles du cycle hydrologiques de celles occasionnées par les changements climatiques et les impacts anthropogéniques s'avère aussi un défi fréquemment souligné (Jung et al., 2010; Koutsoyiannis, 2020; Wu et al., 2013). Un approfondissement des connaissances sur le phénomène de l'évaporation et de la manière de l'estimer est donc nécessaire, notamment le développement d'une méthode standardisée pour effectuer des analyses à grande échelle.

Les facteurs influençant l'évaporation

L'eau nécessite de l'énergie pour changer de la phase liquide à gazeuse. L'énergie disponible dans la colonne d'eau est donc une des deux composantes principales contrôlant le taux d'évaporation d'étendue d'eau, la deuxième étant la diffusion de la vapeur d'eau vers l'atmosphère. C'est d'ailleurs pourquoi la littérature s'intéressant aux facteurs influençant l'évaporation de surface d'eau libre se concentre sur l'effet de 4 variables : La température de l'air, le taux d'humidité, la vitesse du vent, et les radiations nettes à la surface de l'eau (Finch et Calver, 2008). Les radiations nettes sont la différence entre les radiations à ondes courtes entrantes et sortantes (radiations solaires) additionnée de la différence entre les ondes à ondes longues entrantes et sortantes (radiations thermiques) entre la surface de l'eau et l'atmosphère (Lenters et al., 2005). Elles dépendent donc de différents facteurs tel que l'angle d'incidence des radiations solaires, l'albédo de la surface de l'eau, la température de l'eau et la météo locale (Cogley et al., 1979; Fogarty et al., 2018; Houser 2006). Les autres sources d'énergie de la colonne d'eau, c'est-à-dire la rétention de chaleur, l'énergie sensible et l'advection d'énergie (débits entrants et

sortants, écoulement et ruissellement, glace et neige), sont moins bien représentée dans la littérature et souvent considérée négligeables bien que cela ne soit pas nécessairement le cas (Blanken et al., 2011; Sturrock et al., 1992; Trenberth et al., 2009). L'influence de la température de l'air, du vent et du taux d'humidité sur l'évaporation se fait par l'intermédiaire du déficit de pression de vapeur entre la surface de l'eau et l'atmosphère. L'évaporation est proportionnelle à ce déficit, donc tout facteur ayant un effet sur la pression de vapeur de l'air ou de l'eau de surface aura un effet sur l'évaporation (Dingman, 2015). La quantité de vapeur d'eau dans un volume d'air dépend de sa température. On peut donc s'attendre à ce que l'évaporation varie en fonction des changements de la température de l'eau de surface et de la température de l'air. La vitesse du vent influence également la pression de vapeur de l'air au-dessus de la surface et a donc un effet possible sur les taux d'évaporation (McVicar et al., 2012).

Bien que l'on puisse soutenir que le climat et la météo soient les principaux responsables de l'évaporation et que notre connaissance des mécanismes derrière ces interactions est déficiente, nous n'avons pas de contrôle sur ceux-ci. D'un autre côté, il est possible de contrôler les caractéristiques physiques d'un réservoir lors de sa conception et sa construction. Les effets de celles-ci sur le taux d'évaporation seraient vraisemblablement indirects, mais sont tout de même intéressants pour la construction de futurs réservoirs. Par exemple, la profondeur et la superficie d'une étendue d'eau influencent la rétention de chaleur de celui-ci, cette dernière étant elle-même une composante importante de l'énergie disponible pour l'évaporation (Blanken et al., 2011). L'analyse de l'effet de ces caractéristiques sur l'évaporation est pratiquement absente de la littérature (Friedrich et al., 2018). De plus, la comparaison des résultats de ces quelques études s'avère complexe, étant donnée l'utilisation de méthodes d'estimation différentes. Par exemple, une étude montre un important changement des flux de surface en faisant varier la transparence de l'eau, la profondeur et l'albédo d'un lac à l'aide d'une interface de modélisation (Subin et al., 2012), mais une autre étude conclue une absence de sensibilité à la profondeur, toujours en variant celle-ci dans un modèle (Wang et al., 2014). Autrement, des études mentionnent l'effet de la profondeur, la superficie, le volume et la transparence sur l'évaporation, mais sans preuves à l'appui (Lenters et al., 2005; Wang et al., 2018; Woolway et al., 2020 à titre d'exemples). Les mécanismes proposés sont généralement fondés sur des présomptions ou sur la physique théorique, ce qui n'est pas idéal (Dingman, 2015). Une analyse approfondie de ce type de caractéristiques est donc impérative et pourrait fournir des indications pour la conception de réservoirs à empreinte eau et pertes d'eau réduites.

Les propriétés physiques d'un réservoir comme la profondeur de la thermocline ou le volume de l'épilimnion sont influencés par la morphologie ainsi que le climat local (Gorham et Boyce, 1989 ; Lewis, 1996), mais leur relation avec l'évaporation est aussi absente de la littérature. Ceci est étonnant, puisque la dynamique de stratification d'un réservoir peut être vue comme la compétition entre le vent et le refroidissement de la surface éliminant la stratification et l'apport d'énergie par radiations solaire la supportant (Wüest et Lorke, 2003). L'évaporation joue donc un rôle dans la formation de la thermocline ainsi que son approfondissement. L'entrainement d'eau profonde de l'hypolimnion vers l'épilimnion est un des mécanismes responsables de l'approfondissement de la thermocline (Spigel et Imberger, 1980). Ce processus nécessite de l'énergie cinétique turbulente fournie par les processus de brassage par le vent, de la convection de l'eau ou du cisaillement. La stratification de densité causée par le réchauffement de la surface crée des forces de flottabilité qui empêchent le brassage. En revanche, la convection causée par le refroidissement de la surface induit de la turbulence, facilite le mélange par cisaillement et favorise l'entraînement d'eau pronfonde (Monismith et MacIntyre, 2009). Si l'on considère que la chaleur latente (évaporation) est l'une des composantes les plus importantes du bilan énergétique d'un plan d'eau (Lenters et al., 2005), on peut supposer qu'elle joue un rôle important dans le refroidissement de la surface, et donc dans la formation de la thermocline. L'équilibre entre le vent, le réchauffement, le refroidissement et le cisaillement varie en fonction de la superficie et du climat. Les masses d'eau dans les tropiques ont tendance à être moins stables que dans les climats tempérés, en raison de la différence de densité moindre dans la colonne d'eau causées par des écarts de température étroits (Kling, 1988 ; Lewis, 1996). Il en résulte une thermocline plus profonde que dans les autres climats, pour des plans d'eau similaires. Dans des conditions de vent semblables, l'évaporation est également plus élevée en moyenne dans les tropiques (Choudhury, 1997 ; Miralles et al., 2011), ce qui produit plus de turbulence par convection, une stabilité réduite et une thermocline plus profonde. La superficie agit sur la profondeur de la thermocline par la force du vent et son effet modifié par le « fetch » (Gorham et Boyce, 1989). Les petites étendues d'eau sont plus à l'abris du vent, ce qui cause un « fetch » réduit. Sur les étendues d'eau plus grandes, un « fetch » plus élevé produit plus de turbulences, réduit la stabilité et approfondit la thermocline (Monismith et MacIntyre, 2009). Ultimement, la description de la relation entre la profondeur de la thermocline et l'évaporation est intéressante, car elle pourrait englober les effets de la morphologie, du climat et de la météo tous ensemble.

Objectifs et contributions

En bref, notre compréhension du phénomène de l'évaporation à long terme et grande échelle est fondamentalement incomplète. Une méthode d'estimation applicable dans la majorité des situations est manquante, puis l'identification et la description des effets de caractéristiques physiques des réservoirs sur leur taux d'évaporation sont négligées. La présente étude a pour but de pallier ces deux lacunes.

Le premier chapitre s'attarde au développement d'une méthodologie qui permet la modélisation et la comparaison efficace de taux d'évaporation d'étendu d'eau libre, applicable dans la majorité des situations. Les défis associés à l'application d'une telle méthode se résument comme suit : (i) Obtenir une grande quantité de données météorologiques à haute fréquence temporelle et à de multiples endroits, (ii) obtenir les données de température de l'eau à cette même fréquence et aux mêmes endroits, puis (iii) s'assurer que les données obtenues soient standardisées pour pouvoir adéquatement les comparer. Pour résoudre ces problèmes, je propose d'utiliser des données de réanalyse météorologique combinées à de la modélisation physique de la température de l'eau à titre de remplacement de données *in situ*. Cette manière de procéder est décrite explicitement puis validée contre des données mesurées en temps réelle provenant de deux différents réservoirs dans deux différentes régions. Cette analyse représente un premier pas vers la conception d'une méthode d'estimation standardisée pouvant interpréter les tendances historiques à grande échelle et prédire celles du futur. Elle constitue une opportunité pour l'amélioration d'outil de gestion et de prévention de risques associés à la pénurie en eau.

Le deuxième chapitre vise à utiliser la méthodologie du premier chapitre pour effectuer une analyse à l'échelle globale. Les évaporations annuelles de multiples réservoirs dispersés alentour de la planète ont été modélisées puis mises en relation avec les différentes caractéristiques physiques de ces derniers. La théorie et la logique m'ont amenée à prédire que l'énergie disponible pour l'évaporation soit un facteur limitant du processus de l'évaporation. Sans la disponibilité de cette énergie, la présence de conditions idéales pour la diffusion de la vapeur d'eau vers l'atmosphère serait insuffisante. Conséquemment, je me suis attendu à identifier une relation importante avec toutes caractéristiques ayant un effet potentiel sur la distribution d'énergie dans le système. Plus précisément, les effets de la profondeur, la superficie et la profondeur de la thermocline ont été explorés. Cette initiative a d'abord pour but d'accroitre notre compréhension du phénomène de l'évaporation. De plus, elle pourra permettre

d’améliorer notre capacité de gestion de ressources hydriques en appuyant la conception de réservoirs à perte d’eau et empreinte eau réduite.

CHAPITRE 1

Combining Climate Reanalysis And Physical Lake Modelling Into A Multi-Model Approach To Estimate Open-Water Evaporation With Limited Data Availability

ABSTRACT

Although eddy covariance is considered the most accurate method for direct measurement of open-water evaporation, its complex and costly nature encouraged the development of countless estimation methods. Most methods are only effective in specific situations, making comparisons between different studies and upscaling analysis difficult. In this study, such a method was developed, but applicable for most water bodies around the globe, even with limited or absent data availability. Our approach consists of combining climate reanalysis and physical lake modelling to compute an energy budget and an aerodynamic equation for estimating evaporation. Both equations were first validated when driven by *in situ* meteorological data, against measured evaporation rates by eddy covariance over two different reservoirs with contrasting morphologies and in different climates. Performances of both equations were good, with RMSEs varying between 0.85 and 1.75 mm day^{-1} and R coefficients, from 0.75 to 0.86. The multi-model approach consisting of averaging the outputs of both equations improved results at both reservoirs significantly, with RMSEs of 0.99 and 0.78 mm day^{-1} and R coefficients of 0.83 and 0.93 . When driven by climate reanalysis inputs, the performance of the multi-model approach was slightly lower, with RMSEs of 1.05 and 0.98 mm day^{-1}, and R coefficients of 0.68 and 0.84. A sensitivity analysis revealed modelled net radiations and wind speeds to be the most inaccurate climate reanalysis components. Their measurement could improve evaporation estimates but was not deemed necessary for good accuracy. Modifications like modelling temporal variability of water albedo, k_d and water level and remote sensing of ice phenology and morphology are suggested to improve our methodology. Overall, our results suggest this approach to be an important contribution, as it could be applied to estimate evaporation of reservoirs that are difficult to access, don't have meteorological stations or to predict evaporation of future impoundments.

1.1 INTRODUCTION

While the concept of supply and demand is at the core of economics, it is easy to forget that it does not necessarily apply to natural resources. Annual freshwater consumption has never stopped rising since 1900. It has now increased nearly six-fold (Ritchie and Roser, 2017), but the water supply has not increased in any way and theoretically never will (Friedrich et al., 2018). It is estimated that already 4 billion people experience severe water scarcity for at least a month each year, and 0.5 billion experience it all year round (Mekonnen and Hoekstra, 2016). Consequently, there is a need to develop better water management and risk assessment tools related to water scarcity. In this matter, the concept of "water footprint" is gaining popularity, which measures the freshwater consumed or polluted by a product, process, business or other entity for its production or operation. Hoekstra and Mekonnen (2011) estimated the water footprint of humanity at 9087 billion cubic meters of water per year, for the decade spanning 1996 to 2005. 11% of this footprint was attributed to open-water evaporation. This highlights the fact that actual freshwater supplies, i.e., lakes and reservoirs, have their own water footprint through evaporative water losses. The quantification of these losses has shown itself to be quite challenging.

The eddy covariance method is widely considered the most accurate method to measure open-water evaporation directly. This method relies on the measurement of turbulent fluctuations of water vapour, which are very fast and changes in concentrations over time are usually small. This requires sophisticated instruments, a lot of care in setting them up and complex data processing. For these reasons, field campaigns using eddy covariance towers tend to be either short in duration or only cover small areas (Burba and Anderson, 2010). Alternatives to direct measurement of evaporation have been proposed in the form of different models and estimation methods, but there is no consensus on a standardized method that can be used accurately for any water body, in any setting (McMahon et al. 2013). As a result, a lot of the literature concentrates on method testing and model performance on individual lakes rather than observing patterns across space and time. Most studies use different methods, resulting in difficult comparisons and results that don't necessarily agree with each other (McMahon et al., and references therein, 2013; Singh and Xu, 1997). All in all, large-scale studies of open-water evaporation are lacking in the literature.

Estimation methods mostly fall into two categories: the aerodynamic (mass transfer) and the energy budget approaches. The former is derived from Fick's law of diffusion, Prandtl-von Kármán universal velocity distribution and Dalton's ideal gas laws applied to water vapour (Dalton, 1802). The data

requirements of this family of methods are low compared to others, as it needs measurements of only wind speed, air temperature, surface water temperature and humidity. However, the drying power of air is described by an empirical wind function using calibrated constants which need to be calculated from measured evaporation rates. Also, the functions take a lot of different forms, each applicable only in specific situations (Singh and Xu, 1997). Universal functions have been proposed but they come with increased errors and uncertainty (McJannet et al., 2012). In contrast, the energy budget methods estimate evaporation as the residual of all energy components needed to close the energy budget of a water body. It has historically been considered the most accurate method and is frequently used as a reference to which other methods are compared to or calibrated with (Finch and Calver 2008; Rosenberry et al. 2007; Winter et al. 1995). Wang and Dickinson (2012) also argued that it was more accurate than eddy covariance measurements, potentially because the latter does not measure fluctuations over the full range of turbulent eddy sizes. The challenges of this method are the large number and frequency of measurements needed for good accuracy. The heat storage term is also hard to estimate because frequent water temperature profiles are needed for its calculation. Care must be used when using this method as errors and uncertainty of individual energy components are added up to the final evaporation rates (Finch and Calver, 2008).

For these estimation methods to be practical for hydrological applications, observational meteorological data must be readily available. This might be the case for developed reservoir complexes and lakes in urban settings, but not for those in remote places and areas of projected impoundments. There are ways to estimate different meteorological parameters in these contexts, but they come with their own caveats. One possible way is to use data from a distant land-based meteorological station. However, work on the subject generally agrees that to obtain reasonable accuracy, net radiations and changes in heat storage still need to be measured *in situ* (Winter et al., 1995). Using aerodynamic methods removes the need for thermal surveys, but wind speed tends to be heterogenous over small distances which leads to decreased accuracy in evaporation rates (Fournier et al., 2021; Oke, 1987). In the absence of observational data, modelling can be used to estimate individual meteorological components. This approach adds considerable uncertainty to final evaporation values, but this is inevitable in the context of limited data availability.

In summary, a more standardized evaporation estimation method applicable in diverse settings is still lacking in the literature. The resulting inability to upscale analysis or to compare results from different

studies together hinders our progress toward a more complete understanding of the evaporation process. In this study, we propose a framework that resolves the challenges associated with limited data availability and is applicable for most lakes and reservoirs around the globe. The workflow to estimate open-water evaporation consist in the combination of climate reanalysis datasets with physical lake modelling. The performance of this methodology was tested against eddy covariance observations taken over two different reservoirs with contrasting morphologies and in different climates. The equations used were first evaluated when driven by on-site meteorological observations to attest to their validity. They were then tested with data from climate reanalysis and physical lake modelling, to emulate the context of a remote water body without available observational data. A sensitivity analysis was performed by replacing alternatively meteorological observations with their climate reanalysis equivalent, to describe errors and uncertainty caused by individual components. Finally, limitations and opportunities for improvement of the proposed methodology were discussed.

1.2 METHODS

1.2.1 Study sites

Two reservoirs with contrasting morphologies and climates were selected to validate the proposed methodology. Their main characteristics are presented in table 1.1 and detailed in the following sections.

Table 1.1 Reservoir's location, morphology, characteristics, and climatology (Chanudet et al., 2015; Descloux et al., 2014; Fournier et al., 2021)

		Reservoirs	
Characteristics	**Units**	**Nam Theun 2**	**La Romaine 2**
Coordinates		17.71°N 105.26°E	50.67°N, 63.25°W
Mean depth	(m)	8	42
Max depth	(m)	39	120
Surface area	(km^2)	489	86
Mean annual secchi depth	(m)	2.09	3.00
Mean annual air temperature	(°C)	23.1	-1.3
Mean annual precipitations	(mm)	2432	990
Köppen-Geiger climate classification		Am	Dfc

1.2.1.1 La Romaine 2

La Romaine 2 (RO2) is situated in the boreal region of Northern Quebec (Canada). The Canadian boreal region is characterised by subarctic to cold continental climates. It has short moist summers and cold, long, and dry winters. Annual variability in weather is strong, as well as seasonal variability. RO2 covers a relatively small area (86 km^2) and is the deepest of both reservoirs with a maximum depth of 120 m (average depth of 42m). Mean annual temperature and precipitations are – 1.3 °C and 900 mm, respectively, with the coldest month being typically January and July, the warmest one. The reservoir is typically frozen from early December to late May (Fournier et al., 2021).

(a) La Romaine 2 (b) Nam Theun 2

Figure 1.1 Satellite images of study sites with location of the eddy covariance tower: (a) La Romaine 2, QC (Canada), (b) Nam Theun 2, Khammouane (Laos)

1.2.1.2 Nam Theun 2

Nam Theun 2 (NT2) is a hydroelectric reservoir situated in the tropical region, in Laos (Khammouane province). This specific region is characterized by a sub-tropical monsoon climate, which has 3 distinct seasons: warm-wet (June to October), cool-dry (November to February) and warm-dry (March to May). NT2 has a surface area of 489 km^2, with an average depth of 8 m (maximum of 39 m). Secchi depth is on average 2.09 ± 0.15 m (Chanudet al. 2015; Descloux et al. 2014). Annual average rainfall from 1995 to 2013 was 2432 mm, with the maximum recorded precipitation being 390 mm day^{-1} (in 2011) during the warm-wet season. The mean annual temperature is 23.1 °C (12 to 30 °C since 2008) with April being the warmest month and January, the coldest.

1.2.2 Field measurements and data processing

1.2.2.1 La Romaine 2

Evaporation measurements at RO2 covered the period of June 2018 to May 2021. The eddy covariance tower was set up on the southern shore of the reservoir. It consisted of the combination of a gas analyzer and sonic anemometer (Irgason, Campbell Scientific), measuring water vapour concentrations at a frequency of 10 Hz. Other meteorological components were measured as well, notably wind speed and direction (05103, R.M. Young), solar radiations (CNR4, Kipp and Zonen) and surface water temperature (UTBI-001, Onset TidbiT v2, HOBOware). A second eddy covariance tower with similar instruments was installed on a floating raft, directly on the reservoir. This tower had the additional advantage of measuring outgoing radiations. However, it could only be deployed during ice-free seasons to prevent damage associated with ice formation. A vertical chain of thermistors attached to a buoy was deployed in the vicinity of the flux towers, providing periodic water temperature profiles up to a depth of 15 m (UTBI-001, Onset TidbiT v2, HOBOware). More details about the instrumental setup can be obtained from Fournier et al. (2021).

Raw 10 Hz measurements were processed with the EddyPro software (LI-COR Biosciences) at 30-min time steps. Operations for data correction and quality control were performed and are described broadly in Fournier et al. (2021). Additionally, gaps in evaporation time series were filled using Reichstein et al. (2005) marginal distribution technique modified for latent heat fluxes. Details of this technique are described extensively in supplementary materials of Fournier et al. (2021). Hourly rates were subsequently summed to a daily time scale for use in the present study.

1.2.2.2 Nam Theun 2

At NT2, the eddy covariance system was installed in an open water area of the reservoir. Data used in this study covers the periods of May 22nd to 28th of 2009 and March 13th to 21st of 2010. Data were acquired at a frequency of 10 Hz by a sonic anemometer (Windmaster Pro, Gill Instruments) and gas analyzer (DLT-100 FMA, Los Gatos Research). A meteorological station was set up on-site for measurements of wind speed and direction, atmospheric pressure, air temperature and relative humidity (Weather Transmitter, model WTX510). Solar radiations (CNR1, Kipp and Zonen) and surface water temperature (Pt100 sensor) were also measured (Deshmukh et al., 2014). Periodic thermal surveys (Quanta multi-probe meter, Hydrolab) were performed at different times during the eddy covariance tower deployment (Chanudet et al., 2015).

Raw 10 Hz data was processed at 30-min time steps using the EdiRe software (Clement, 1999). Data correction and quality control operations were performed on eddy covariance data and are described extensively by Deshmukh et al. (2014). Gaps in evaporation time series were filled using the same methodology as RO2, i.e., the marginal distribution technique modified for latent heat fluxes by Fournier et al. (2021). As for RO2, hourly rates were subsequently summed to a daily time scale.

1.2.3 Climate reanalysis

Climate reanalysis from ERA5 (Copernicus Climate Change Service, 2017) was used in the second part of this study, to replace actual measurements of meteorological data in the computation of evaporation estimation equations and the modelling of water temperature. ERA5 is the fifth-generation atmospheric reanalysis of global climate by the European Centre for Medium-range Weather Forecast (ECMWF). It provides hourly estimates of numbers of climatic variables, covering Earth on a horizontal $30km^2$ grid on 137 levels of vertical resolution, up to a height of 80km. Data is available from 1979 onwards, within 3 months of real-time. ERA5 combines observational data, advanced modelling, and data assimilation systems to provide climate reanalysis datasets (Hersbach et al., 2020). The reanalysis dataset "ERA5-Land hourly data from 1981 to present" was used for the present study. It was produced through models driven by near-surface atmospheric fields from ERA5, with thermodynamical orographic adjustment of temperature and lapse-rate correction of other components (Muñoz-Sabater, 2019). These modifications to the ERA5 basic dataset added the benefit of an increased spatial resolution of $9km^2$. Details of the reanalysis variables used for this study are available in supplemental materials (appendix A).

1.2.4 Water temperature modelling

Water temperature profiles are necessary for the computation of some evaporation estimation equations, but these were not continuously available for both reservoirs. Consequently, physical lake modelling was used to estimate daily water temperature profiles. We used the Simstrat 1D physical lake model, a one-dimensional physical lake model for the simulation of deep lake stratification and mixing developed at the Swiss Federal Institute of Aquatic Science and Technology (Eawag). It uses a k-ε energy closure scheme for turbulent mixing and includes internal energy transfer via internal seiches (Goudsmit et al. 2002). Its accuracy was demonstrated on multiple water bodies in different settings (Gaudard et al., 2017, 2019) and is regularly reviewed and updated. The model was executed through R Studio (R core team 2020) with the "LakeEnsemblR" library (Moore et al. 2021).

To simulate a temperature profile, Simstrat requires a minimum of water body bathymetry, meteorological data (wind speed, humidity or dewpoint temperature, air temperature, atmospheric pressure, incoming solar radiations) and light extinction coefficient (k_d). More data can also be included for increased accuracy (see Moore et al. 2021). For the first part of this study, Simstrat was executed with as many measured inputs as possible. When measured data was not available, climate reanalysis was used to fill the gaps. In the case of RO2, meteorological inputs were all measured during ice-free periods. In addition, incoming longwave radiations (radiant heat) were available, so they were added to the model, although not mandatory. An annual average Secchi depth of 3.0 m was estimated by Rust and al. (2022), which was converted to a k_d of 0.5 m^{-1} to be used in the model. At NT2, meteorological data was also available except for atmospheric pressure. Chanudet et al. (2014) measured a Secchi depth of 2.09 ± 0.15 m, which was converted to a k_d of 0.7 m^{-1}. For both reservoirs, water and ice albedo were set to constant values of 0.08 and 0.9, respectively, because they were not monitored. Simstrat requires the input of the fraction of seiche energy to total wind energy. Because this was not available at both sites and was challenging to estimate, its value was determined by Latin hypercube calibration (See Moore et al., 2021). These calibrations were made against available thermal surveys. Accurate hypsography was not available at both reservoirs and was estimated according to Imboden (1973). Details of this method are available in supplemental materials (appendix C). For the second part of this study, simulations were executed a second time with climate reanalysis inputs only, to emulate the context of a remote water body without available measurements. The light extinction coefficient was set to a constant arbitrary value of 1.0 m^{-1} and the seiche parameter to 0.01, as proposed by Simstrat's documentation as a typical value.

1.2.5 Evaporation estimation methods

Despite the efforts made in developing better hydrological models, no single model can be judged superior in describing processes under all conditions (Beven, 2006; Duan et al., 2007). Thus, multi-model analysis is often preferred, as it adds confidence to modelled results (Fritsh et al., 2000). Here we estimated evaporation with two different methods with different theoretical backgrounds. We also evaluated the performance of averaging the rates estimated by both methods as a third estimate of evaporation. This last method will be designed as a "multi-model average" for the remaining of this article.

1.2.5.1 Bowen Ratio Energy Budget method

The Bowen Ratio Energy Budget (BREB) method is based on the law of conservation of energy. It accounts for incoming, outgoing, and stored energy in a system. It can be expressed as follow (Lenters et al. 2005):

$$N = R_n + A_n + G_n - H - L,$$

where *N* is heat storage of the water body, R_n is net radiation at the water surface, A_n is net advected energy, G_n is net energy exchange between the sediments and overlying water, *H* is sensible heat flux and *L* is latent heat flux. By rearranging this equation, evaporation (*E*) can be derived from latent heat (*L*) and water's latent heat of vaporisation (λ):

$$L = \lambda E,$$

$$E = \frac{R_n + A_n + G_n - H - N}{\lambda}.$$

The sensible heat flux term cannot be determined readily unless there are instruments in place to perform direct measurements. Bowen (1926) developed a method to describe the ratio of sensible to latent heat, termed the Bowen ratio (β). A modified form to obtain β without direct measurement of sensible heat was developed (Brutsaert 2013):

$$\beta = \frac{H}{L} = \frac{c_p \emptyset (T_s - T_a)}{\varepsilon_m \lambda (e_s^* - e_a)},$$

where c_p is the specific heat of air at constant pressure, $\emptyset$ is the atmospheric pressure, T_s and T_a are temperatures of the water surface and the air, ε_m is the ratio of molecular weight of water to that of dry air, e^*_s is saturation vapour pressure at water surface temperature and e_a is the vapour pressure of the overlying air. The ratio $c_p \emptyset / \varepsilon_m \lambda$ is also termed the psychrometric constant, γ. By substitution, we can eliminate the sensible heat term in the first equation and obtain the following, which constitutes the BREB method:

$$E = \frac{R_n + A_n + G_n - N}{\lambda(1 + \beta)}.$$

The exchange of energy in a water body is usually governed by exchanges at the water surface and heat storage in deep lakes (stratified), rather than advected energy and sediment conduction (Henderson-sellers, 1986). For shallow lakes, sediment conduction can however be significant (Sturrock et al. 1992).

Thus, the final equation was simplified to the following, termed reduced energy budget (Finch and Calver, 2006):

$$E = \frac{R_n + G_n - N}{\lambda(1+\beta)}.$$

Details of the computation of individual energy budget components are available in supplemental material (appendix D).

Daily evaporation rates estimated by the BREB method were inspected and modified to meet certain quality criteria. Evaporation values are problematic when the Bowen ratio (β) is close to -1 (Irmak et al. 2014). This is clear from the formulation of the last equation, where a β close to -1 would cause an inaccurately large evaporation value. This usually happens in pseudo-adiabatic conditions, where the saturation mixing ratio is close to the specific humidity of the air (Savage et al. 2009). Therefore, evaporation rates were rejected when β was between -1.3 and -0.7, as recommended by Kurc & Small (2004).

1.2.5.2 Mass transfer

The mass transfer method used in this study is an integral part of the Simstrat physical lake model. It estimates free-water evaporation with an equation based on Dalton's law (Dalton, 1802), which relates evaporation to wind speed and the vapour pressure deficit between the water surface and the atmosphere. It takes the form of:

$$E = f(u)(e_s^* - e_a),$$

where *f(u)* is a wind function describing the drying power of air, e^*_s is saturation vapour pressure at water surface temperature and e_a is the vapour pressure of the overlying air. The wind function used is the Ryan-Harleman equation (Ryan et al., 1974), with modifications proposed by Adams et al. (1990):

$$f(u) = \sqrt{(2.7\Delta\theta^{1/3})^2 + (3.1U)^2},$$

where $\Delta\theta$ is a term accounting for the increase in driving buoyancy force by evaporation and U is wind speed. This equation gives more weight to the second term, i.e., forced convection (wind-driven) than the first term, free convection (buoyancy driven) in the process of evaporation. It is advantageous in the context of modelled water temperature since errors in modelled temperature will have less effect on evaporation rates. When ice cover is expected, the equations are switched. Simstrat simulates lake ice

formation and decay according to Leppäranta (2010, 2014) and Saloranta and Andersen (2007), which propose to use a variation of the mass transfer equation, i.e., a bulk transfer equation. The bulk transfer formula is expressed as:

$$E = k_c U(q_s - q_a),$$

where k_c is the bulk exchange coefficient, U is wind speed, q_s is specific humidity at the water surface q_a is specific humidity of the air. The bulk exchange coefficient can be considered constant at 1.5 x 10^{-3} according to recommendations in Leppäranta (2010). For more details regarding the different equations, parameters and their computation, readers are referred to Simstrat's documentation (available freely on "Eawag – Applied System Analysis" GitHub), Goudsmit et al. (2002) and Schmid and Köster (2016). For the ice module specifically, see Gaudard et al. (2019).

1.2.5.3 Multi-model average

Multi-model averaging has received a lot of attention in the atmospheric and hydrological literature (Beven et al., 2006; Diks and Vurgt 2010; Duan et al., 2007). The idea behind this approach is that combining multiple models each with its weaknesses and strengths is at least as good as individual models. This form of model selection has been shown to reduce errors and uncertainty in modelling environmental processes (Diks and Vurgt, and references therein, 2010). Taking this into consideration, we evaluated the performance of a third approach to estimate evaporation, in the form of multi-model averaging. Given its simplicity and because we expected the BREB (energy budget) and mass transfer (aerodynamic) methods to be complementary, we used the equal weights averaging method, where each model output is weighted equally.

1.2.5.4 *In situ* VS climate reanalysis inputs

In the first part of the study, we evaluated the validity of the estimation methods. To do so, the estimation equations were with *in situ* observational data from eddy covariance towers, except water temperature which was estimated via physical modelling. The second part of the study computed the equation with the best performance but with climate reanalysis inputs only. This was done to evaluate its practical application in the context of remote water bodies without available observational data.

1.2.6 Performance analysis

Four different metrics were used to describe the performance of the estimation methods and the water temperature modelling. Mean absolute error (MAE) expresses the overall agreement between observed and modelled values, in real units. Every deviation is given the same weight, regardless of the sign. The root mean squared error (RMSE) is essentially the same as MAE, but the squared parameter gives more weight to modelled values with large deviations from observed values. Comparing RMSE and MAE indicates the presence of outliers. The mean bias error (MBE) is a signed metric in real units which indicates a model's tendency of over or underestimation (Dawson et al., 2007). However, it needs to be used with other metrics since positive and negative errors cancel each other out. Finally, the linear correlation coefficient (R) indicates the tendency of modelled values to oscillate similarly to observed values through time.

1.2.7 Sensitivity analysis

A sensitivity analysis was carried out by replacing alternatively each measured meteorological component used in the estimation equations with its climate reanalysis equivalent. The performance of each substitution was analyzed and compared to the performance of the equations with all *in situ* inputs. The objective of this exercise was to determine where the largest errors are likely to come from and whether it would be recommended to measure some of the meteorological components for adequate estimation of evaporation rates.

1.3 RESULTS AND DISCUSSION

1.3.1 Estimation of water temperature profiles

For RO2, the calibrated seiche parameter for the years 2018 and 2019 were 0.0011 and 0.0058 respectively, and of 0.0035 for the years 2020 and 2021. For NT2, the parameter was calibrated to 0.0022 and 0.0018 for the years 2009 and 2010, respectively. With calibrated a_{seiche} and k_d, modelled temperature profiles showed reasonable agreement for both reservoirs, except for the year of 2009 at NT2 (table 1.2; figures B1 and B3, Appendix B). This specific simulation overestimated water temperature during the stratified period and couldn't reproduce adequate mixing events during fall (figure B3a, Appendix B). For both reservoirs, replacing *in situ* observations with climate reanalysis and omitting the calibration led to a significant loss in performance (table 1.3). For RO2, the overall temperature changes over time maintained the same dynamics, but the simulated depth of the thermocline was always too shallow and surface water

temperature during stratified periods was mostly overestimated (table 1.3a; figure B2, Appendix B). For the simulation of NT2, water temperature across the water column was overestimated, the thermocline depth was too deep, and the reservoir stratified too early (table 1.3b; figure B4, Appendix B). These losses of performance were inevitable since the distribution of energy in the water column is major driver of water temperature (Monismith and MacIntyre, 2009). However, we argue that the performance is still acceptable in its context. Further analysis confirmed the adequate estimation of evaporation rates without calibration of water temperature (section 1.3.3).

Table 1.2 Parameters and performance of Simstrat calibrated simulation of water temperature with *in situ* meteorological inputs.

Modeled year	**a_{seiche}**	**k_d (m^{-1})**	**RMSE (°C)**	**MBE (°C)**	**MAE (°C)**	**R**
(a) La Romaine 2						
2018	0.0011	0.5	1.616	-0.405	1.358	0.98
2019	0.0011	0.5	1.594	0.170	1.236	0.97
2020	0.0058	0.5	1.046	-0.022	0.773	0.98
2021	0.0035	0.5	1.953	-1.178	1.269	0.98
(b) Nam Theun 2						
2009	0.0022	0.7	2.311	-0.571	1.609	0.79
2010	0.0018	0.7	0.868	0.663	0.092	0.95

Note: a_{seiche} is the fraction of seiche energy to total wind energy and k_d is the light extinction coefficient (m^{-1}).

Table 1.3 Performance of Simstrat's uncalibrated simulation of water temperature with climate reanalysis meteorological inputs.

Modeled year	**a_{seiche}**	**k_d (m^{-1})**	**RMSE (°C)**	**MBE (°C)**	**MAE (°C)**	**R**
(a) La Romaine 2						
2018	0.01	1.0	3.597	-1.122	2.521	0.87
2019			2.666	0.585	1.757	0.92
2020			2.980	1.374	1.951	0.91
2021			3.517	1.770	2.572	0.90
(b) Nam Theun 2						
2009	0.01	1.0	2.589	1.620	2.116	0.84
2010			3.057	2.785	2.787	0.90

1.3.2 Estimation of daily evaporation with on-site measurements

Comparison of measured evaporation rates by eddy covariance and estimated rates with *in situ* meteorological inputs is shown in figure 1.2 and 1.3. Their performance metrics are shown in table 1.4.

1.3.2.1 Bowen ratio energy budget method

The accuracy of the energy budget methods at the daily timescale has often been questioned. That is because evaporation rates at that scale were shown to be driven by wind speed and atmospheric stability (Assouline and Mahrer, 1993) and because errors accumulate from each term when calculating a residual. We show here that reasonable estimates can still be obtained with observed meteorological measurements and modelled thermal profiles of the water column. The BREB method yielded good performance overall. The errors and bias are relatively low in all cases. The correlation coefficients at both sites are good, indicating a good capacity to reproduce the variability of evaporation rates over time (table 1.4).

Table 1.4 Performance of estimation methods in estimating daily evaporation rates using daily averaged *in situ* meteorological inputs.

Estimation method	RMSE (mm day^{-1})	MAE (mm day^{-1})	MBE (mm day^{-1})	R
(a) La Romaine 2				
BREB	1.24	0.97	-0.32	0.75
Mass transfer	0.95	0.64	0.01	0.80
Multi-model average	0.99	0.76	-0.19	0.83
(b) Nam Theun 2				
BREB	0.85	0.70	0.37	0.86
Mass transfer	1.75	1.64	-1.64	0.86
Multi-model average	0.78	0.67	-0.64	0.93

The RO2 time series had a lot of gaps which came in part from missing meteorological observations and inadequate Bowen ratio values. Different methods to fill gaps in heat fluxes time series are available, but they were not used here because the goal was to assess the performance of BREB's direct estimates only. The MBE at RO2 is relatively low, but we expect from the visualization of the time series that if there wasn't any missing data point, the negative bias would be more important (figure 1.4a).

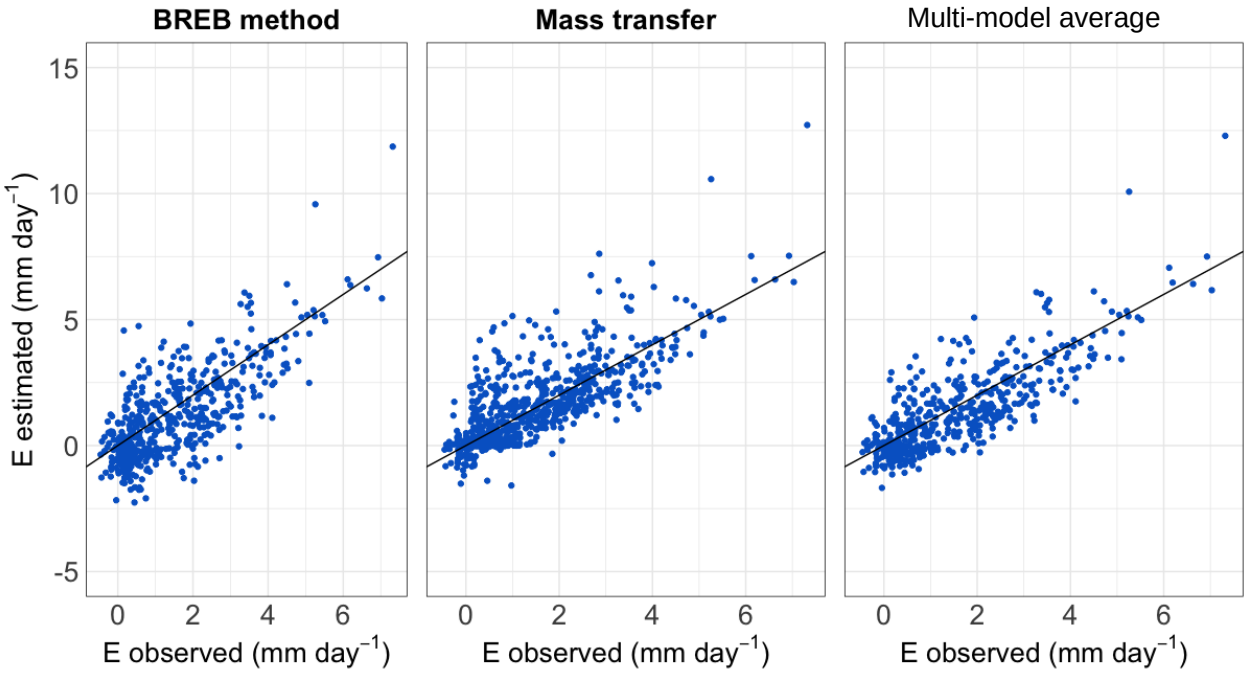

Figure 1.2 Comparison of daily measured evaporation rates and estimated evaporation rates with *in situ* meteorological inputs at La Romaine 2. 1:1 line is represented by the black lines.

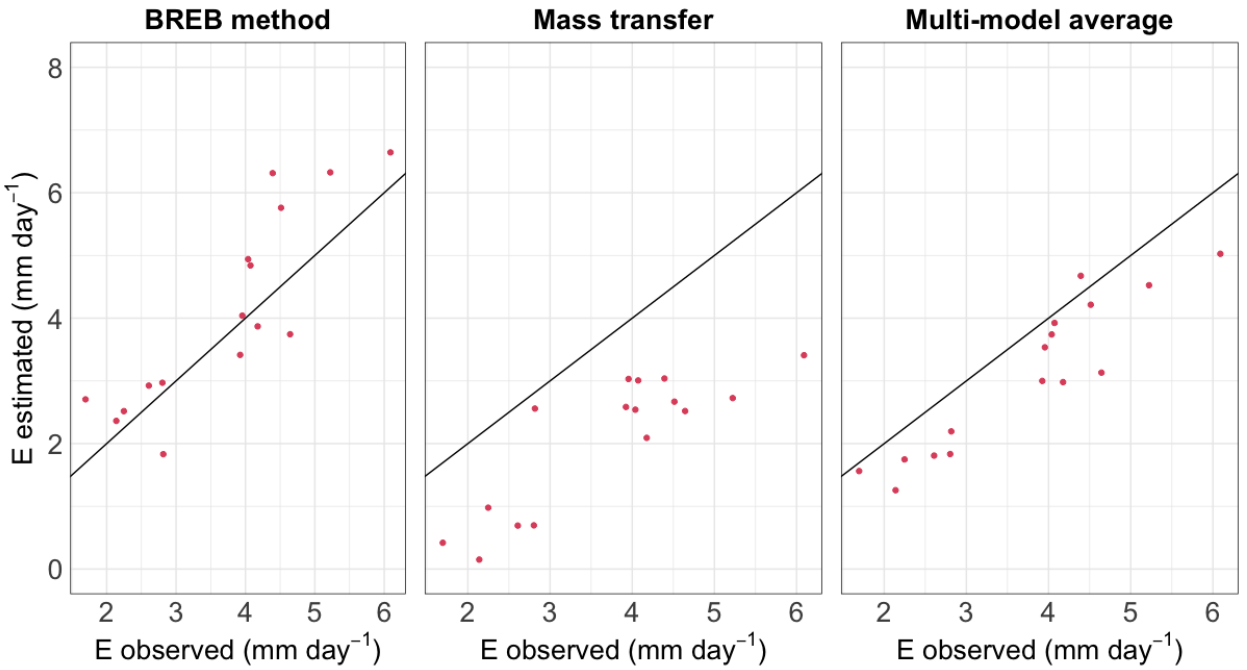

Figure 1.3 Comparison of daily measured evaporation rates and estimated evaporation rates with *in situ* meteorological inputs at Nam Theun 2. 1:1 line is represented by the black lines.

Its negative value indicates an overall tendency to underestimate evaporation (table 1.4a). This seems to be due to the period of late spring to early summer, where the modelled rates are always lower than the observed rates. We did not consider ice phenology in our computation of the BREB method, which might be in part responsible for these errors. Ice on RO2 usually breaks up around this period, in late May. When ice is melting, most of the energy from incoming radiations is used for warming the water column (Leppäranta, 2014). This leaves little energy available for evaporation and rates remain low. Then, evaporation rates start to rise gradually as the surface water temperature gets near its annual maximum. The magnitude of these rates depends in part on incoming radiations but also on changes in heat storage of the water body (Lenters et al., 2005). These changes are usually slower after ice break-up (Leppäranta, 2014). Since water temperature was modelled, the omission of ice cover in our calculations might have overestimated changes in heat storage, resulting in lower evaporation rates. Additionally, we cannot account for the accuracy of modelled temperatures at depths deeper than 15 m, because thermal surveys were only conducted up to that depth. The changes in temperature at these depths could have a significant impact on heat storage estimation, especially at times of reservoir turnover and early stratification, when temperature changes are happening in the whole water column (Lenters et al., 2005). The uncertainty in our modelled heat storage may have brought some errors in evaporation rates, but it can be seen as a better option than omitting the term altogether, as other studies have shown a more important loss of performance when doing so (Gan and Liu, 2020). It would also explain why model performance was better at NT2 as well as why we didn't obtain the same negative bias. Indeed, this reservoir doesn't develop an ice cover, and the heat storage variability of tropical reservoirs is generally low (Sene et al., 1991).

A contribution to bias and errors at both reservoirs could be the omission of advected energy in the energy budget equation. Watershed runoff is an important source of advected energy, even more so when ice and snow are melting (Siemens et al., 2021). Peaks of inflow to the reservoir can also lead to controlled withdrawals from the reservoir (Huokuna et al., 2022). The combination of inflows and outflow can influence evaporation rates through available energy, which would be missing in this study.

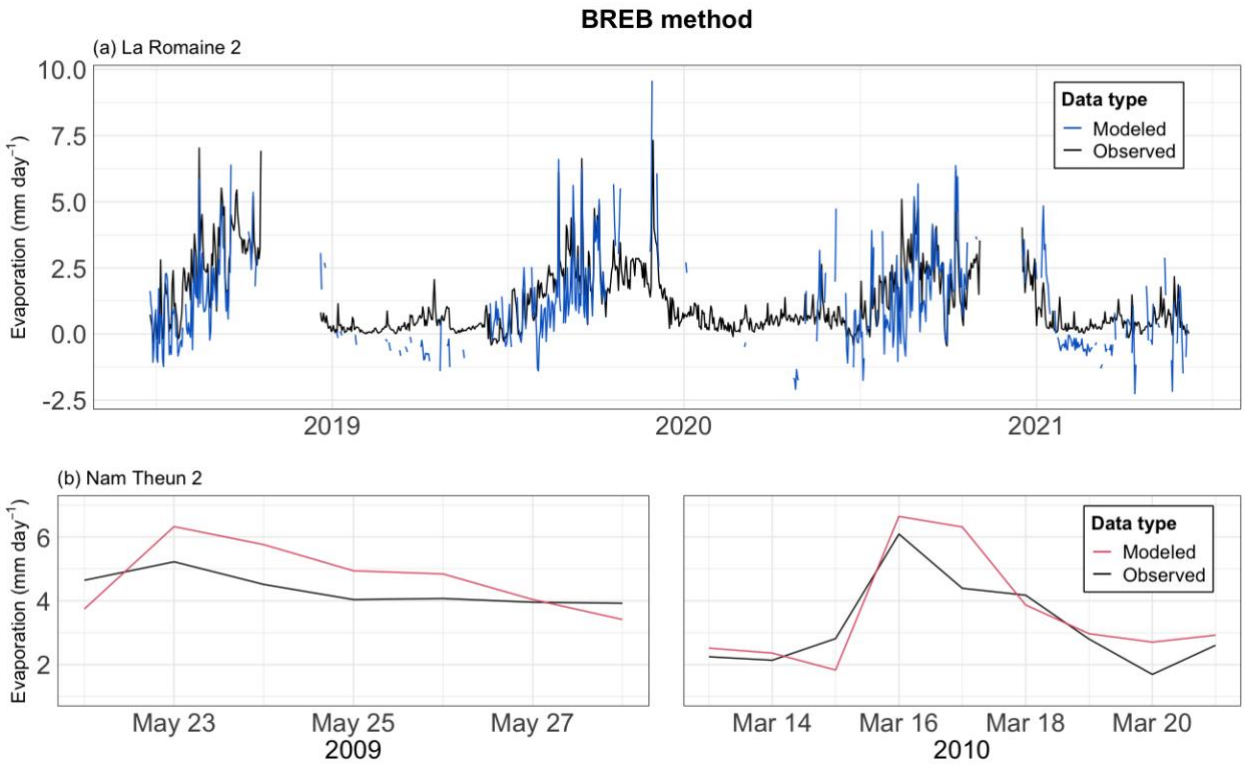

Figure 1.4 Daily measured and modeled evaporation time series computed with the BREB method using *in situ* meteorological inputs.

1.3.2.2 Mass transfer

The performance of the mass transfer method was slightly lower than the BREB method at NT2 and slightly better at RO2 (table 1.4). The estimated evaporation rates at NT2 varied similarly to observed rates, as indicated by its high correlation coefficients. However, they were all underestimated, resulting in a high negative MBE (figure 1.5b; table 1.4b). The mass transfer equation with modifications by Ryan et al. (1974) and Adams et al. (1990) describes the evaporation process as driven by forced (wind-driven) and free (buoyancy-driven) convection, with more weight given to forced convection. Thus, it is unlikely that a large underestimation of evaporation rates results from inaccurate modelled water surface temperature

(Majidi et al., 2015). It could be that the adjustment of wind height of 10 to 2 meters resulted in the underestimation of wind speeds.

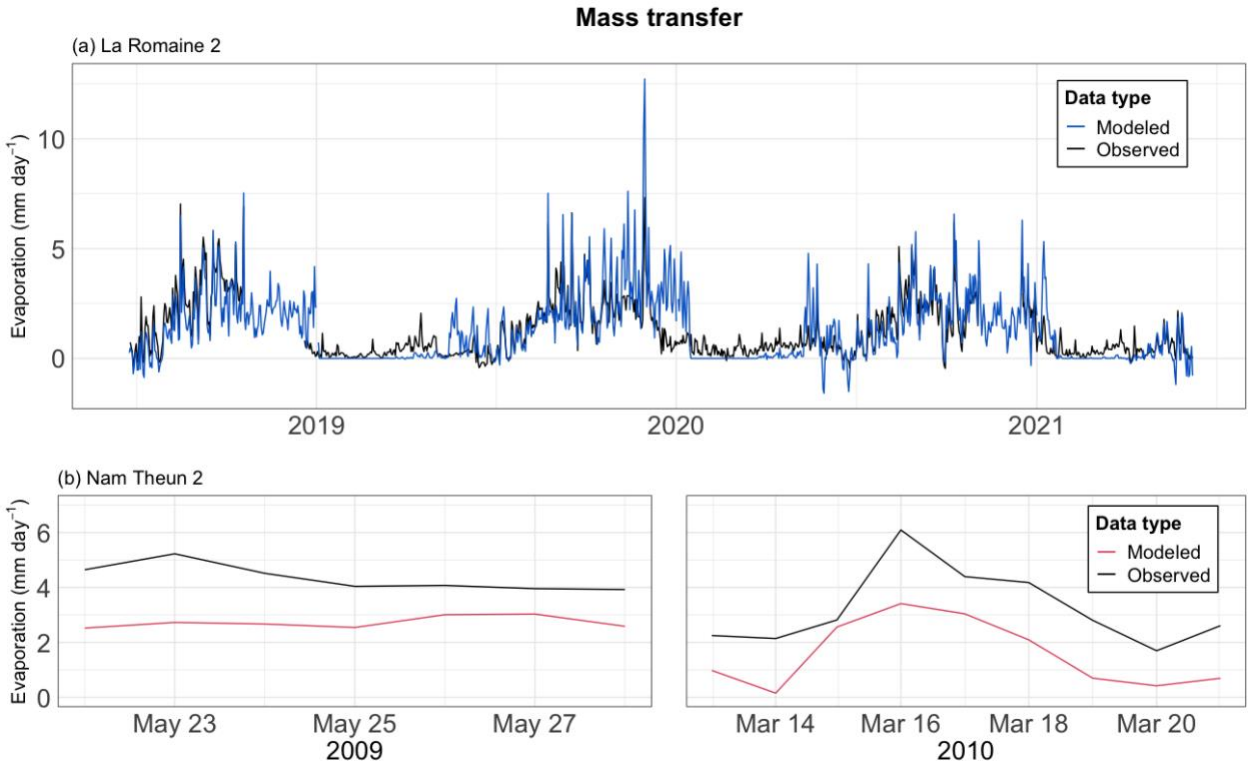

Figure 1.5 Daily measured and estimated evaporation time series computed with the mass transfer method using *in situ* meteorological inputs.

Simstrat uses a constant roughness height in the conversion of its wind speed (see Simstrat's documentation). While this is usually recommended for water surfaces (Dingman, 2015), it does not necessarily reflect reality. Since mass transfer equations are sensible to wind speed variations (Fournier et al., 2021; Singh and Xu, 1998), such an assumption inevitably reduces the accuracy of modelled evaporation rates. There wasn't a similar underestimation at RO2. The performance of the mass transfer method at this reservoir was overall good, with an average bias of almost zero. This seems to be the result of some abnormally high rates in 2019 combined with an overall small underestimation of other rates (figure 1.5a). The difference between MAE and RMSE hints at the presence of some outliers in the dataset, which is visible in figure 1.2. Estimated evaporation rates during winter were almost always null (figure 1.5a) when ice cover was expected by the Simstrat ice module. In this situation, most incoming energy is assumed to be reflected in the atmosphere, while retained energy is lost in ice and snow melting (Leppäranta, 2014). This leaves little to no available energy for evaporation and explains the low rates in

winter, but null rates are unlikely and were indeed never observed in this study. The loss of performance caused by the null rates is probably negligible since their equivalent observed rates are low, but modifications to the ice module to accurately estimate evaporation and sublimation rates in the winter are still an improvement opportunity.

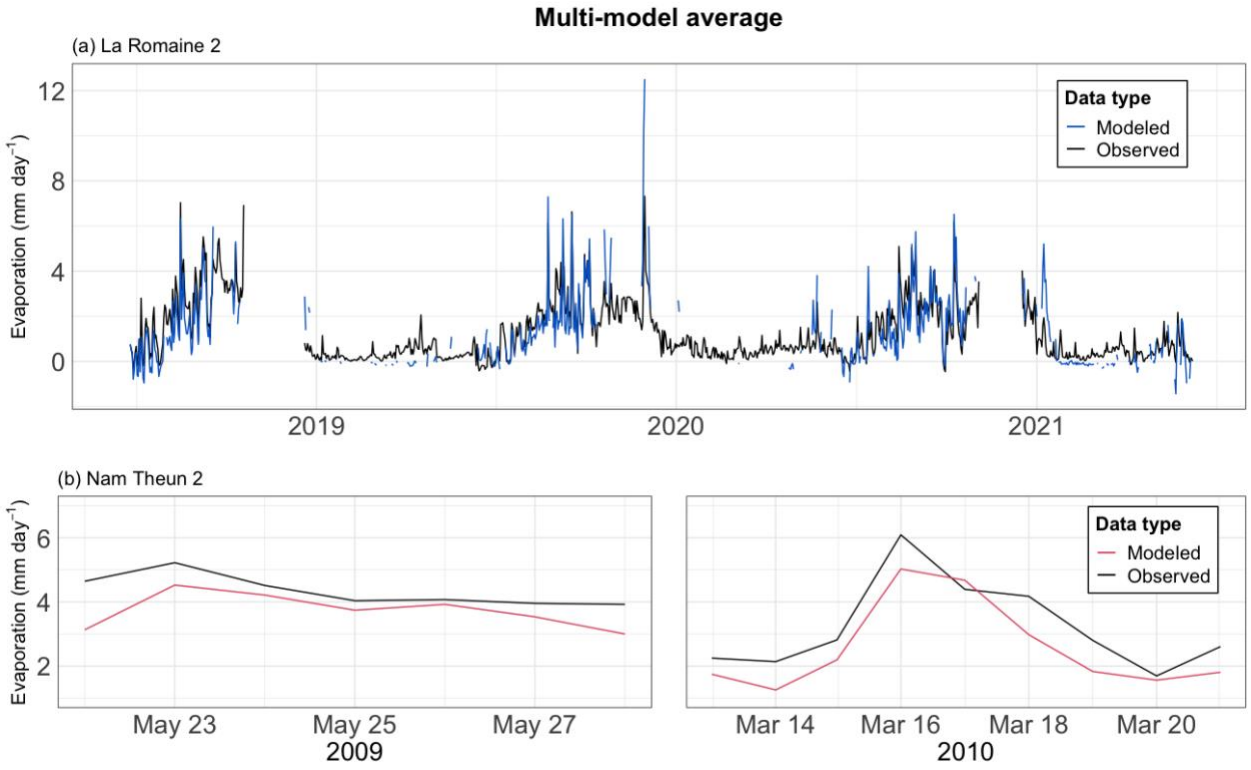

Figure 1.6 Daily measured and estimated evaporation time series computed with the multi-model average method using *in situ* meteorological inputs.

1.3.2.3 Multi-model average

The multi-model average had the best performance of all methods at NT2 and a similar performance to the mass transfer method at RO2 (table 1.4). The improvement at NT2 is visible in figures 1.2 and 1.6, especially in the ability of the model to reproduce variability over time. Even if the performance metrics were similar at RO2, we can see an improvement in figure 1.2, with data, and points more regularly dispersed around the 1:1 line. This is also shown by an improvement in the correlation coefficients (table 1.4). The improvements can be explained in part by the balancing effect of underestimations from the BREB method and overestimations from mass transfer estimates, although probably not that simple. This balancing effect can sometimes be the result of overlapping differences in the sign of errors in individual components of the modelling equations (Fritsch et al., 2000). We believe it

was also attributed to the combination of an aerodynamic and an energy budget method. This idea is not new. It is the basis of a family of methods termed "combination equations", with the Penman-Monteith and Priestly-Taylor equations being some of the most widely used evaporation estimation methods (Finch and Calver, 2006). This family of equations was developed to encompass the advantages of both energy budget and mass transfer methods and overcome their individual challenges. However, they are often found less accurate than the other more data-intensive methods (Finch and Calver, 2008; McMahon et al., 2013) and frequently less accurate than mass transfer methods (Fournier et al., 2021; Wang et al., 2019). They especially fall short when dealing with deep water bodies, as the heat storage term becomes larger (Finch and Calver, 2008). The multi-model average used here is more data-intensive but retains all the advantages of combination equations without its drawbacks. Aerodynamic methods relate evaporation to wind speed and the vapour pressure deficit between the water surface and the atmosphere. However, evaporation cannot happen without sufficient available energy (Assouline and Mahrer, 1993; Sene et al., 1991), something not considered in this family of methods. The energy budget methods, on the other hand, estimate evaporation as a residual energy component. Assuming this component adequately represents the actual evaporation rate implies ideal conditions for the process to happen, which is not always true. Both methods have their theoretical shortcomings but complement each other. We hypothesize here that the improved performance of the multi-model average is derived from this complementarity.

1.3.3 Estimation of daily evaporation with climate reanalysis data

To evaluate the practical application of the proposed methodology in the context of remote water bodies without available observational data, evaporation was estimated with meteorological inputs from climate reanalysis exclusively (ERA5). Considering it gave the best results at both sites, we used only the multi-model average method for this section. The time series of modelled rates compared to observational eddy covariance rates are shown in figure 1.7, and the performance metrics, in table 1.5. Overall, the performance metrics all stayed in good ranges. When compared to the performance of the same method with observational data, the RMSE and MAE were slightly higher at both sites. The MBE of RO2 was slightly higher but still in a good range (-0.33) while it kept the same magnitude at NT2 (0.64), but with reversed sign (table 1.5b). The correlation coefficients had the biggest drops in performance, with values going from 0.83 to 0.68 and from 0.93 to 0.84 for RO2 and NT2, respectively.

.

Table 1.5 Performance of the multi-model average method in estimating daily evaporation rates using climate reanalysis daily averaged meteorological inputs.

Meteorological inputs	RMSE (mm day^{-1})	MAE (mm day^{-1})	MBE (mm day^{-1})	R
(a) La Romaine 2				
In situ	0.99	0.76	-0.19	0.83
Climate reanalysis	1.05	0.80	-0.33	0.68
(b) Nam Theun 2				
In situ	0.78	0.67	-0.64	0.93
Climate reanalysis	0.98	0.82	0.64	0.84

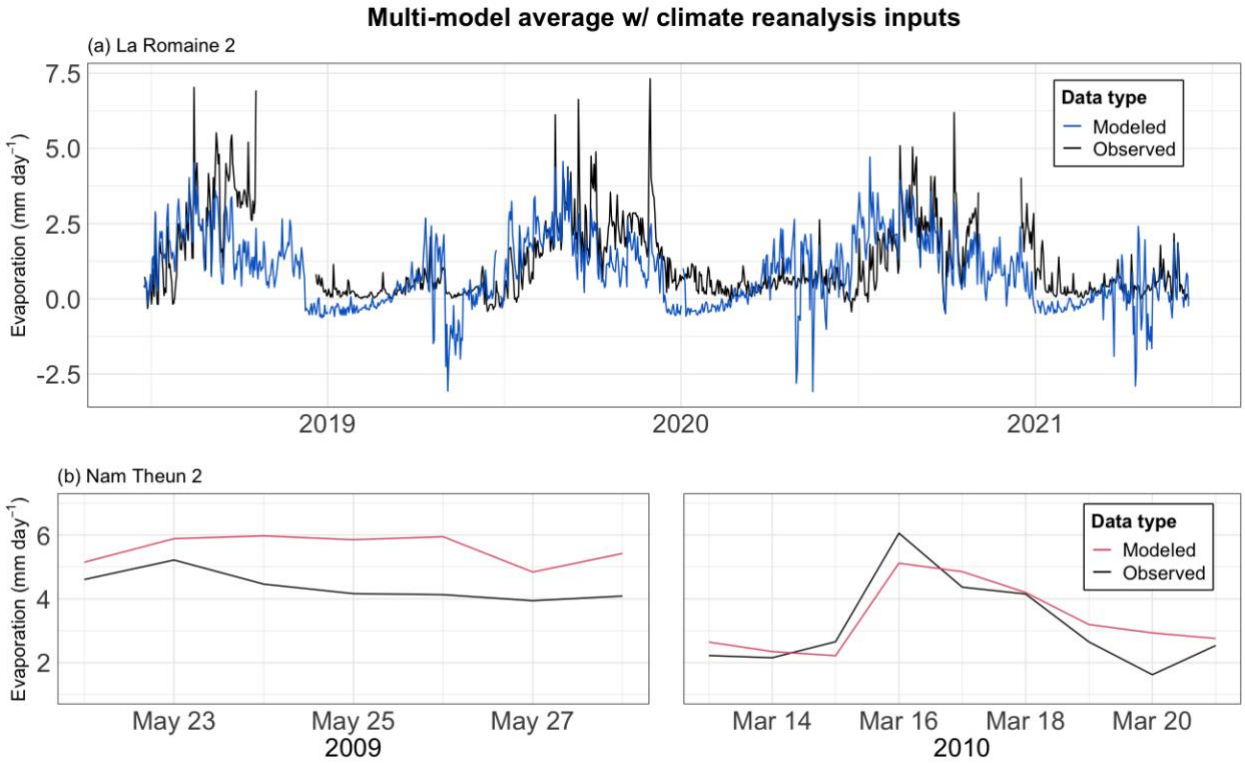

Figure 1.7 Daily measured and estimated evaporation time series computed with the multi-model average method using climate reanalysis meteorological inputs.

The shortwave radiations modelled by ERA5 at NT2 tended to be overestimated (figure 1.8b). This could explain why changing meteorological data from measurements to climate reanalysis resulted in such a change in MBE at NT2. Higher incoming shortwave radiations at the water surface without any changes in other meteorological variables translated into higher net radiations (figure 1.9b), which would cause an

overestimation of modelled evaporation rates from the BREB method. Still at NT2, wind speeds from ERA5 had a good correlation with measured speeds but had the tendency to be underestimated (figure 1.8b). Lower wind speeds would result in underestimated evaporation rates from the mass transfer equation which would theoretically produce smaller performance metrics when combined with the overestimation of shortwave radiations. However, this is not what we observed here (table 1.5b). ERA5 modelled variables are interpolated over 9 km^2. Because wind speed is highly variable over small distances and heterogenous landscapes (Oke, 1987), wind speeds from climate reanalysis may be more appropriate than *in situ* measurements for estimating evaporation of a large surface. This also highlights that measuring wind speed over a single point can result in the erroneous estimation of average speed over the full water body. Therefore, we argue that loss of performance would mainly be from the overestimation of the BREB method. At RO2, the same underestimation of wind speeds is observed, but without a drastic change in MBE (figure 1.8a; table 1.5a). The ERA5 shortwave radiations at RO2 were more tightly confined around the 1:1 line than at NT2. Therefore, the lower evaporation rates from underestimated wind speeds would not be compensated by the BREB method in the same way.

There was a systematic overestimation of ERA5 dewpoint temperatures under 0°C at RO2 (figure 1.8a). The eddy covariance tower at RO2 was situated on the shore, where humidity levels might differ from nearby land (Condie and Webster, 1997), while ERA5 provides humidity levels over a 9 km^2 area. Averaging dewpoint temperature over an area with a heterogeneous landscape might have caused the observed overestimation. Also, it is unclear whether ERA5 considers dewpoint temperature under zero degrees Celsius as frost point temperatures or not. If they did, it would contribute to the overestimation since frost point temperatures are always higher than dewpoint (Leppäranta, 2014). Dewpoint temperature is linked to water vapour in the atmosphere. At constant air temperature, a higher dewpoint indicates more water vapour and a higher vapour pressure. Thus, an overestimation of dewpoint temperatures is expected to cause smaller vapour pressure deficit and smaller evaporation rates. This is reflected in the negative MBE (table 1.5a).

Evaporation rates at RO2 during ice cover were underestimated and there was irregular variability at times of ice break-up (figure 1.7a). Our approach might not be accurate during ice periods since we did not consider ice phenology in our calculations of the BREB method. For instance, we used constant albedo and latent heat of evaporation for the BREB method, but ice has as a much higher albedo than open water which results in higher reflection of solar radiations and less available energy at the water surface (Wang

et al. 2018). Also, sublimation requires more energy than evaporation (Leppäranta, 2014). This coincides with high variability in modelled net radiations when measurements were around zero (figure 1.9a), which is expected from the reflection of most of the incoming solar energy. Both these assumptions would result in underestimated evaporation rates.

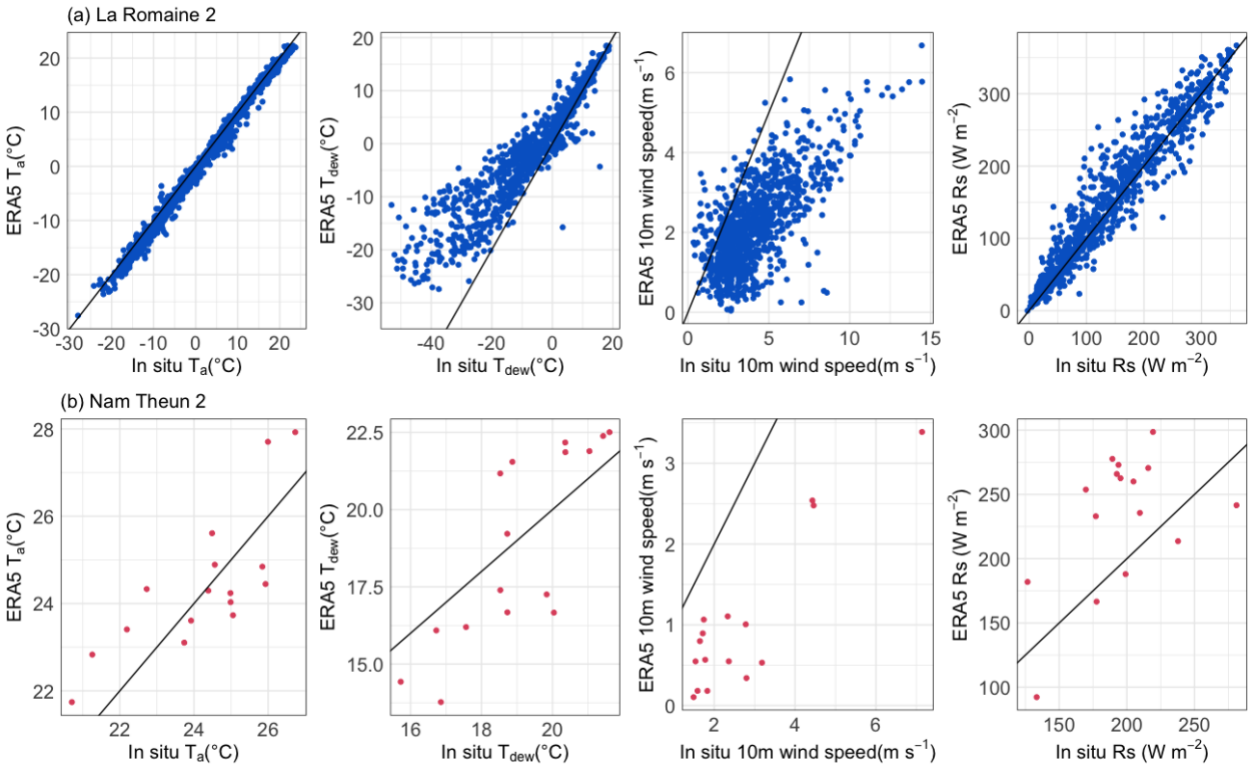

Figure 1.8 Comparison between *in situ* and climate reanalysis (ERA5) meteorological inputs. T_a is air temperature, t_{dew} is dewpoint temperature and R_s is incoming shortwave radiations. 1:1 line is represented by the black lines.

The change of phase of water at freezing or thawing times induces a change in energy allocation (Trenberth et al. 2009). This creates irregular changes in surface water temperature which translate into high variability in the heat storage component of the BREB method. Fournier et al. (2021) obtained a similar variability during the early summer period and attributed it to the use of a constant bulk transfer coefficient, which does not adequately represent the reduced efficiency of vapour transport by atmospheric turbulence caused by stable atmospheric conditions at those times. This might also explain the reduced correlation coefficients at NT2 since atmospheric conditions are generally more stable in tropical climates (Seidel and Yang, 2020). Also, there were a lot of gaps in observational data at RO2 during periods of ice cover which prevented us to compare evaporation rates at those times. It is possible that

the performance of this method would have been lower without these gaps, and a smaller loss of performance would have been obtained when replacing measurements for climate reanalysis.

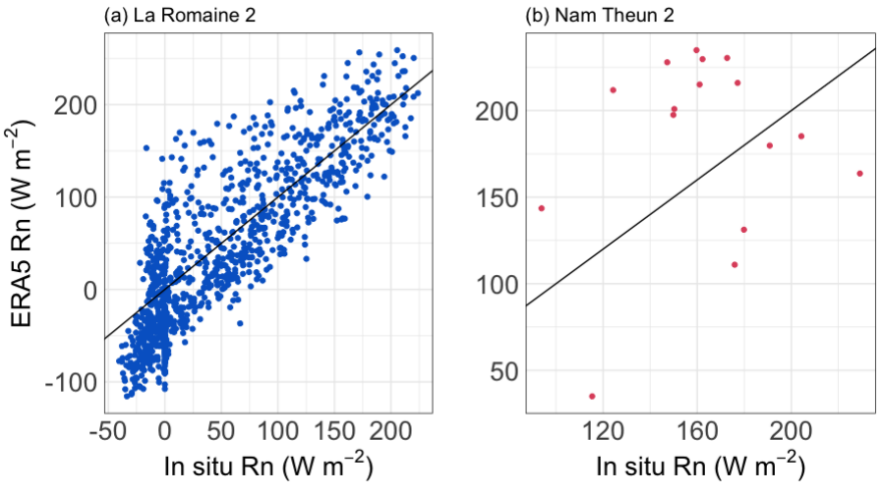

Figure 1.9 Comparison between measured and modeled net radiations at the water surface (R_n). 1:1 line is represented by the black lines.

1.3.4 Sensitivity analysis

A sensitivity analysis was performed by replacing alternatively measured meteorological components with its climate reanalysis (ERA5) equivalent in the multi-model average method. Doing so helped describe the effect of individual climate reanalysis inputs on the method performance. Substitution of air temperature did not change performance in a significant way (table 1.6). There was a good agreement between measured and ERA5 air temperatures, with data points tightly confined around the 1:1 line (figure 1.8a). Dewpoint temperature substitution also did not change the performance of the estimation method significantly (table 1.6). This is surprising for RO2 since there was a systematic overestimation of dewpoint temperature under zero degrees Celsius (figure 1.8a). The air humidity level is a determinant factor of the evaporation process, as indicated by both the BREB and the mass transfer equations. However, negative dewpoint temperatures happened in winter, when evaporation rates are small because of weaker solar radiations and the presence of ice cover. Thus, resulting discrepancies between measured and modelled rates might not have influenced performance significantly. The comparison of dewpoint temperatures over zero degrees Celsius was better, when evaporation rates are expected to be higher (figure 1.7a). Climate reanalysis dewpoint temperatures at NT2 were in good agreement with the measured temperatures (figure 1.8b). This substitution caused a small loss of

performance, with higher MBE and MAE (table 1.6b). These changes were of the order of 0.10 and 0.17 mm day^{-1} (3 and 5% of mean daily evaporation rate), which can be considered negligible.

Table 1.6 Performance of the multi-model average method in estimating daily evaporation rates with substitution of single measured meteorological component for its climate reanalysis (ERA5) equivalent.

Meteorological inputs	RMSE (mm day^{-1})	MAE (mm day^{-1})	MBE (mm day^{-1})	R
(a) La Romaine 2				
All *in situ* inputs	0.99	0.76	-0.19	0.83
ERA5 T_a	0.95	0.73	-0.19	0.82
ERA5 T_{dew}	1.01	0.76	-0.15	0.78
ERA5 R_n	1.06	0.78	-0.20	0.78
ERA5 wind speed	1.03	0.79	-0.11	0.83
All ERA5 inputs	1.02	0.77	-0.23	0.76
All ERA5 inputs w/o calibration	1.05	0.80	-0.33	0.68
(b) Nam Theun 2				
All *in situ* inputs	0.78	0.67	-0.64	0.93
ERA5 T_a	0.71	0.63	-0.57	0.93
ERA5 T_{dew}	0.70	0.80	-0.67	0.93
ERA5 R_n	1.11	0.87	0.29	0.80
ERA5 wind speed	0.92	0.67	-0.44	0.77
All ERA5 inputs	0.98	0.76	0.21	0.82
All ERA5 inputs w/o calibration	0.98	0.82	0.64	0.84

Note: T_a is air temperature, T_{dew} is dewpoint temperature and R_n is net radiations at the water surface. Calibration consists in setting the light extinction coefficient to its measured value instead of a generic value of 1 and estimating the seiche parameter by Latin hypercube calibration in the simulation of water temperature profiles, rather than using a generic value of 0.01. See methods section 1.2.5 for details.

The substitution of net radiations (R_n) resulted in the biggest loss in performance at NT2. RMSE and MAE were significantly higher, the MBE had its sign reversed and the correlation coefficient dropped from 0.93 to 0.80 (table 1.6b). Almost half of modelled daily R_n were underestimated (figure 1.9b). R_n is the central component of the BREB method, and our results show that errors in its estimation have the biggest impact on the estimation of evaporation rates, even with a multi-model approach. R_n variability is similar to R_s variability (figure 1.8b). Hence, solar radiation variability seems responsible for evaporation rate variability. Overall, the performance of the method with modelled R_n was still in an acceptable range.

We hypothesize that combining the BREB and mass transfer methods helped limit performance losses. If higher accuracy is needed, measuring R_s might best help in keeping errors in estimated rates low. In contrast, a comparison between modelled and measured R_n and R_s at RO2 showed a more balanced pattern around the 1:1 line (figures 1.8 and 1.9). This explains why the substitution of R_n at RO2 did not produce such a loss in performance.

Wind speed substitution at NT2 resulted in the second lowest performance. The MBE and MAE did not change significantly, but the RMSE was higher. The correlation coefficient was the lowest of all substitutions, but at a reasonable value of 0.77. In comparison, the same substitution at RO2 did not make a big difference in performance (table 1.6). At both sites, climate reanalysis wind speeds were underestimated (figure 1.8a). At NT2, the evaporation rates estimated by the mass transfer were already significantly lower than the observed rates (table 1.4b). An added underestimation of wind speeds would result in even lower rates and would explain the obtained performance. At RO2, the initial mass transfer method had a better performance, which was similar to the BREB method (table 1.4a). We believe this is the reason the substitution of wind speed did not impact the multi-model average the same way. Overall, none of the substitutions had a dramatic impact on the method performance. We conclude that climate reanalysis data is a good alternative to on-site measurements. It's interesting to note that it gave better results than using data from distant, land-based meteorological stations in other studies (Fournier et al.,2021; McJannet et al., 2012). Interpolating data over a large area might help in limiting errors caused by high variability of weather over short distances and heterogeneous landscapes.

Comparison between the calibrated and uncalibrated multi-model average method with climate reanalysis inputs helped us describe how much performance would be lost from unavailable light extinction coefficient (k_d) and thermal surveys for adjusting the fraction of seiche energy to wind total energy parameter (a_{seiche}) in Simstrat's modelling interface. These two variables had the potential to affect both estimations methods used in the multi-model average since k_d influences the absorption of solar energy and a_{seiche} influences the distribution of energy throughout the water column (Goudsmit et al., 2002; Kirk, 1985). These changes in the energy budget would impact directly different components of the BREB method, and indirectly on the mass transfer method by changes in water temperature and vapour pressure at the water surface. Our results show a minor loss of performance from the uncalibrated modelling of evaporation rates (table 1.6), even if calibration significantly improved the accuracy of modelled water temperatures (table 1.2 and 1.3). It is reasonable to assume that errors in a given

evaporation rate come from incorrect interpretation of either an energetic or an aerodynamic process, but rarely from both at the same time. We hypothesize that our multi-model approach to estimating evaporation had a buffering effect on systematic errors produced by either of the methods used with uncalibrated k_d and a_{seiche}.

There is inherent uncertainty in climate reanalysis data produced by ERA5 (Hersbach et al., 2020; Muñoz-Sabater, 2019). It provides weather observations when available, but when they aren't, advanced weather forecasting models and spatial interpolation is used. Like any weather forecasting system, this causes uncertainty. However, a certain level of uncertainty may be deemed acceptable in the context we are trying to emulate, that is, remote water bodies, future impoundment areas, or areas without available meteorological observations. Overall, the sensitivity analysis indicated that substituting measured meteorological data with climate reanalysis does not produce large errors in evaporation rates. We conclude that uncertainty and errors in climate reanalysis datasets are sufficiently low to be used for proposed purposes of this study.

1.3.5 Limitations and future work

1.3.5.1 Temporal variability in water characteristics

Water characteristics like reflectivity and light absorbance can vary over time. Suspended particles and coloured dissolved organic matter (CDOM) affect the depth at which solar radiations penetrate in a water body (Kirk, 1985, 1994). In turn, this can affect the amount of absorbed energy, water temperature, and overall energy budget, all factors that drive the evaporation process. These factors can also change the water surface albedo (reflectivity), which directly impacts the amount of absorbed energy by the water body. Water surface albedo at high latitudes also varies through seasonal changes in the angle of incidence of solar radiations (Cogley, 1979). Reflectivity and light absorbance were described by constants in this study and were used in different parts of the modelling process. This represents a limitation of our modelling approach that brings errors and uncertainty in estimated evaporation rates. Work could be done in the future to adequately describe temporal changes in water physical characteristics and improve overall modelling performance. Another characteristic that was considered constant is the water level. Changes in water level caused by inflows and outflows can change the volume of water in a reservoir significantly. The water level at NT2 for example can vary by up to 9.5 meters seasonally, corresponding to a variation in the reservoir surface area from 168 to 489 km^2 (Deshmukh et al., 2014). This would affect

the heat storage component of the BREB method, which is computed as the sum of energy contained in discretized layers of reservoir water volume. Modelling inflows and outflows and including water level variations would consequently improve the accuracy of estimated evaporation rates. We mentioned already that ice and snow phenology was not considered in our computation of the BREB method. Because ice and snow have a much higher albedo than water and because freezing and thawing events alter the energy budget of a water body, this omission brings errors in estimated evaporation rates and fails to adequately describe temporal variability at these specific times. Thus, future work includes the consideration of ice phenology in the BREB method computation. Possibilities include borrowing the module directly from Simstrat or using remote sensing technology.

1.3.5.2 Spatial variability of evaporation rates

Drivers of evaporation like wind speed, surface water temperature, vapour pressure, depth, albedo, light penetration, and sediment reflection may be variable across a given water body. Consequently, it can't be assumed that estimated evaporation rates over a single point are representative of the whole reservoir. Future work should be done on spatial variability of evaporation rates. Our modelling approach could be modified to estimate this variability to a certain extent. By subdividing reservoirs into sections of a given area, it would be possible to estimate evaporation with consideration of spatial variability in meteorological variables and physical characteristics. This would provide a better estimation of the total evaporation of a water body to be used in subsequent analysis. Also, eddy covariance measurements describe evaporation over a large portion of the reservoir but cannot be considered representative of its whole surface area. The BREB method estimates evaporation according to characteristics of the deepest point of the water body, which might not be equivalent to those around the eddy covariance tower. Therefore, using eddy covariance rates as a benchmark to evaluate the performance of our method might have caused systematic errors and uncertainty.

1.3.5.3 Remote sensing

Remote sensing technology represents an interesting opportunity to improve our methodology. Progress has been made in the last decades on deriving optical and physical properties of water bodies from satellite observations. It was shown that water transparency and reflectivity can be described with good accuracy, by the determination of typical indicators like Secchi depth, k_d, turbidity, CDOM and suspended particulate matter (Dörnhöfer and Oppelt, 2015). As discussed throughout this article, the

addition of specific k_d and surface albedo to our modelling workflow would improve its performance. Since satellite observations are usually available at multiple times throughout a year, the temporal variability of both these variables would also be possible to implement. Bathymetry can also be derived from remote sensing (Giardino et al., 2014a, 2014b). We were able to estimate evaporation rates with reasonable accuracy by simulating water body morphology from the surface area, and maximum and average depth (Imboden, 1973), but specific morphology might improve estimated evaporation rates significantly. It would be particularly helpful when dealing with water bodies of irregular or atypical morphology. Surface water temperature can be determined with reasonable accuracy by remote sensing indicators (Schneider and Hook, 2010). However, care must be taken especially when using aerodynamic methods, as even a small deviation in estimated temperatures can be problematic (Fournier et al., 2021). In the methodology presented in this study, the surface water temperature could be used directly in the mass transfer and BREB equations, and for calibration of Simstrat. The latter would yield a better water temperature estimation of the whole water column and resolve some issues we had with surface water temperature dynamics. This would improve confidence in the evaporation rates estimated by both methods, through more accuracy in the estimation of vapour pressure at the water surface and the heat storage component. Finally, there is an opportunity to describe ice and snow phenology with remote sensing indicators (Arp et al., 2013; Nolin, 2010). Knowing accurately when ice is present on a reservoir would refine our methodology by improving the estimation of the net radiation terms in the BREB method. It would also provide more accurate modelling of changes in the energy budget caused by melting and freezing events. Remote sensing of ice cover could also be used in place of the ice module in Simstrat or to validate its output.

1.4 CONCLUSION

The objective of this study was to develop and validate a method for estimating open-water evaporation applicable for most water bodies around the globe, with limited or absent data availability. We did so by combining climate reanalysis and physical lake modelling to generate the data needed to compute two different equations. The performance of both equations as well as their equally weighted average was evaluated against eddy covariance observations taken over two different reservoirs with contrasting morphologies and in different climates.

The performance of the equations was first evaluated when driven by on-site measured meteorological data, to attest to their validity. Both equations yielded good performances at the daily

timescale. At RO2, the BREB method performance was slightly lower than the mass transfer method, which might be coming from failing to consider advected energy and ice phenology in its computation. At NT2, the mass transfer method did slightly better than the BREB method, because of the absence of ice cover and overall more stable atmospheric conditions in tropical climates. Errors and uncertainty at both reservoirs also came from using simulated water temperature profiles in place of their unavailable measured equivalent at the daily timescale. At NT2, averaging outputs from both equations improved their accuracy. At RO2, it had similar performance metrics to estimated rates by the mass transfer equation, but with better distribution around the 1:1 line when compared with observed rates. We hypothesized these improvements to be derived from the complementarity of an energy budget and an aerodynamic approach for estimating evaporation.

The performance of the multi-model average method was then evaluated when driven by meteorological data from climate reanalysis. There was a significant drop in all performance metrics, but the overall accuracy of estimated rates was still good. At NT2, overestimated shortwave radiations and underestimated wind speeds by climate reanalysis were judged responsible for performance losses. Overestimation of dewpoint temperature under 0°C and energy budget changes occasioned by ice phenology were pointed out as responsible for the losses at RO2. Discrepancies between *in situ* and climate reanalysis meteorological components are believed to be the result of a combination of factors, notably their spatial variability and the location of the eddy covariance towers.

A sensibility analysis was carried out by replacing alternatively each measured meteorological component with their climate reanalysis equivalent. This exercise was done to identify where the largest errors in evaporation rates were coming from and to recommend whether some components should be measured for adequate accuracy. The biggest loss in performance came from the substitution of net radiations at the water surface, followed by the substitution of wind speed. The accuracy of these replacements was still good. Therefore, their measurement was not deemed necessary. Replacing air and dewpoint temperatures did not cause a significant drop in performance. Replacing the actual light extinction coefficient and calibrating the fraction of seiche energy to total wind energy in the Simstrat simulation model caused negligible changes in performance. We conclude that our multi-model approach had a buffering effect on systematic errors produced by either of the methods used for estimating evaporation rates.

Finally, limitations and opportunities for improvements were discussed. Some water characteristics were considered constant like reflectivity and light absorbance, as well as water level. However, they can vary over time, potentially causing inaccuracies in our estimated evaporation rates. Drivers of evaporation may be variable across a given water body, like wind speed, water surface temperature, vapour pressure, depth, albedo, and others. We proposed that modifications to our modelling approach could be done to estimate spatial variability of evaporation rates over a water body, to provide more accurate rates over its whole surface area. Lastly, remote sensing was considered as an alternative to constants and modelled variables and for model calibration, for the overall improvement of our modelling approach.

Overall, the results of our study show that daily evaporation rates can be estimated with easily available *ex situ* meteorological data (climate reanalysis), modelled water temperature profiles (Simstrat) and modelled typical reservoir morphology (by Imboden, 1973) at an accuracy similar to other studies using observational meteorological data (Fournier et al., 2021; Meng et al., 2020). This approach represents an important contribution since the ERA5 reanalysis tool provides data covering the entire planet from 1950 within 3 months of real-time (Copernicus Climate Change Service, 2017). Therefore, the methodology proposed in this study could potentially be applied to estimate the evaporation of reservoirs that are difficult to access, don't have meteorological stations or fill gaps in existing datasets. It is of particular interest to predict evaporation of future impoundments since morphology and temperature are unavailable and meteorological stations might not be present in these areas.

CHAPITRE 2

The Relationship Between Thermocline Depth, Stratification And Annual Evaporation In Reservoirs: A Global Analysis

ABSTRACT

Evaporation from reservoirs represents a substantial loss of freshwater to the atmosphere. The identification and description of relationships between reservoir morphology, physical properties and evaporation are therefore of interest for resources management and risk assessment related to water scarcity. The objective of this study was to detect such relationships, as well finding indicators of evaporation that are easy to measure, estimate or predict, to efficiently predict annual evaporation. To do so, we combined physical lake modelling (Simstrat) and climate reanalysis (ERA5-land) into a multi-model approach to estimate evaporation from 187 reservoirs across the globe. Evaporation rates from reservoirs varied between 152 and 1972 millimeters per year with a mean of 927, and represented on average 6.4% of their mean annual inflow. No relations were found between annual evaporation and surface area, mean and maximum depth. A generalized additive model relating evaporation with thermocline depth and duration of stratification explained 77% of the model's deviance, with an R^2 of 0.76. Annual evaporation was lowest with shallow thermoclines, starting at 2 meters. Evaporation then followed a linear relationship up to 6 meters, where it was at its highest and remained constant for deeper thermoclines. Reduced heat losses from the lowered temperature difference between the water surface and the atmosphere expected from lower thermocline, providing more energy for evaporation, were suggested as an explanation. We also explored the cooling effect of wind and evaporation, causing more turbulence and less stability which would potentially deepens the thermocline. Annual evaporation was highest with a short duration of stratification from 1 day up to 160 days and stabilized at its lowest for longer durations. Reduced stability and density gradient caused by high evaporation rates were suggested as an explanation for this relationship. We concluded that thermocline depth and duration of stratification constitute a good proxy for predicting evaporation from reservoirs. It is easier to measure or predict than actual evaporation, offering an alternative to complex, time-consuming logistics, and encompass the effects of weather and morphology together. We believe that our results can be used to improve water resource management and provide indications on ways to design reservoirs with reduced evaporative water losses and water footprints.

2.1 INTRODUCTION

With a growing world population comes a growing demand for resources. However, a growing demand does not come with growing supplies, and some of the resources we blindly take for granted are slowly becoming scarce. Consumable water is surprisingly becoming one of those. Indeed, it is estimated that 4 billion people experience severe water scarcity for at least a month each year, and 0.5 billion experience it all year round (Mekonnen & Hoekstra 2016). In this matter, the concept of "water footprint" is gaining popularity, which measures the freshwater consumed or polluted by a product, process, business or other entity for its production or operation. Hoekstra and Mekonnen (2011) estimated the water footprint of humanity to be 9087 billion cubic meters of water per year, for the decade spanning 1996 to 2005. 11% of this footprint was attributed to open-water evaporation.

Of particular interest, evaporation from reservoirs represents substantial losses of freshwater. For example, Zhao and Gao (2019) estimated that 33.73 billion cubic meters of water per year were evaporated from 721 reservoirs in the United States from 1985 to 2014 (93% of the annual public water supply in the U.S.A., in 2010). Also, Australia loses about 40% of its total water storage capacity per year to evaporation (Craig et al. 2005) and reservoir evaporation in Texas is equivalent to about 126% of total municipal water use (Wurbs et Alaya, 2014). While it is true that evaporated water does not disappear and eventually comes back as precipitation, it might not be at the right time nor at the right place to compensate for the losses. Water scarcity is an important problem in multiple countries. Moreover, localized depletion has a significant outreach on other parts of the world, as so many countries depend on others for agriculture and food production, water-dependant product manufacturing and energy production, or even for actual drinking water and food supply (Oki & Kanae 2006). Thus, the ability to estimate and predict evaporation from reservoirs is important, as it might affect the availability of consumable water across the globe.

Water needs energy to change from its liquid to its gaseous state (latent heat). Thus, available energy is one of two main components controlling evaporation, the second one being the diffusion of water vapour to the atmosphere. For a given water body, available energy is a combination of net radiation at the water surface, the heat stored in the water column and water-advected energy (Finch & Calver 2008). Net radiation is the amount of energy captured by a water body, from incoming shortwave and longwave radiations. Incoming shortwave radiations vary in their proportion of direct to diffuse portions, depending on different atmospheric properties. This is important because the angle of incidence of

radiations affects the albedo of the water surface (Cogley 1979), which determines the proportion of reflected shortwave radiations. Thus, it has its importance in seasonal variations of evaporation at higher latitudes, where sun elevation varies significantly throughout the year. Stored heat in the water column is used by liquid water as energy to change state and evaporate. Because of its high specific heat capacity, water stores a lot of heat, and its total amount depends mostly on depth. For the same reason, seasonal variations in evaporation rates will vary depending on the depth of the water body (Blanken et al. 2011). Inflows and outflows can contribute significantly to the energy budget of a water body. Inflows consist of groundwater seepage, river flow, surface runoff and precipitations while outflows are rivers discharge, groundwater leakage and evaporation. However, unless the volume of advected water is high compared to the actual water body volume, or if the temperature difference between the advected water and the water body is high, it is usually considered negligible (Sturrock et al. 1992; Sacks et al. 1994). Snow and ice are also sources of advected energy. Change of phase of water at freezing or thawing times induces changes in energy allocation, moving energy from the surface to the atmosphere (Trenberth et al. 2009). Interestingly, Assouline and Mahrer (1993) found that evaporation at a short scale (hourly to daily) is determined primarily by wind speed and atmospheric stability while heat storage and net radiation have more effect on longer timescales (daily and onward). For the latter, energy budget methods are more suitable.

Much of the literature looking at factors influencing open-water evaporation is focused on the effect of 4 variables: Air temperature, humidity, wind speed and net radiation (Finch & Calver 2008). While climate is arguably the biggest driver of evaporation and that much is left to be learned about its effect on it, it is not something we can control. On the other hand, the morphology of a water body is something we can effectively control when we design and build reservoirs. The effect of it on evaporation would most probably be indirect, but they are still of interest for future reservoir impoundments. For example, depth and surface area are known to influence the heat storage of a water body, which is an important component of available energy for evaporation (Blanken et al. 2011). The effect of these on evaporation is practically absent from the literature. When they are addressed, it is frequently based on assumptions or theoretical physics, which is not ideal (Dingman 2015). The lack of large-scale and long-term data is hindering development on this subject. Few studies are addressing this directly, and they are usually based on a single lake or reservoir observations. Comparing the results of different studies together is challenging because of the wide array of measurements or modelling methods. One study has found large surface flux changes when varying water opacity, depth, and albedo of a single lake through a modelling interface

(Subin et al. 2012), but another one inferred a lack of sensitivity to depth, again by varying factors in a model (Wang et al. 2014). Otherwise, studies are quoting the effect of factors like depth, surface area, volume, and colour to name a few, but without any direct supporting evidence (Lenters et al. 2005; Wang et al. 2018; Woolway et al. 2020, to name a few). Proposed processes are usually based on either assumption or derived from theoretical thermodynamics.

Dynamic physical properties of water bodies like thermocline depth and surface mixed layer (SML) volume are influenced both by morphology and local climate (Gorham and Boyce, 1989; Lewis 1996), but their relationships with evaporation are also lacking in the literature. This is surprising since SML dynamics can be seen as a competition between wind energy and surface cooling acting to eliminate stratification, and surface heating (mostly by solar radiations) creating stratification (Wüest and Lorke, 2003). Thus, evaporative cooling must play an important role in thermocline formation (stratification) and SML thickening. One of the primary mechanisms responsible for SML thickening is the entrainment of deeper, denser water from below the thermocline into the SML (Spigel and Imberger, 1980). This process requires turbulent kinetic energy supplied by stirring processes from wind mixing, water convection or shear. Density stratification caused by surface heating creates buoyancy forces that act to suppress turbulent mixing. In contrast, convection caused by surface cooling induces turbulence, facilitates mixing by shear and favors entrainment (Monismith and MacIntyre, 2009). Considering latent heat (evaporation) is one of the largest components in the energy budget of a water body (Lenters et al., 2005), we can assume that it plays a large role in surface cooling, and thus, in SML thickness and formation of the thermocline. The dynamic balance between wind, heating, cooling, and shear varies with surface area and climate. Water bodies in the tropics tend to be less stable than in temperate climates, because of small density differences in the water column caused by narrow temperature ranges (Kling, 1988; Lewis, 1996). This results in deeper thermocline depth than in other climates, for similar water bodies. In similar wind conditions, evaporation is also higher on average in the tropics (Choudhury, 1997; Miralles et al., 2011), causing more turbulence by convection, reduced stability and deeper SML. The surface area acts on thermocline depth through wind stress and its modified effect caused by fetch (Gorham and Boyce, 1989). Small water bodies are more sheltered from the wind, resulting in reduced fetch. On larger water bodies, higher fetch produces more turbulence, reduces stability, and deepens the thermocline (Monismith and MacIntyre, 2009). Ultimately, describing the relationship between thermocline depth and evaporation is of interest, as it might encompass the effects of morphology, climate, and weather altogether.

Overall, the interpretation of the evaporation process over water bodies is still a work in progress. The identification and description of relationships between reservoir morphology, physical properties and evaporation are neglected. In this study, we aimed to detect such relationships. In addition, we sought to find indicators of evaporation that are easy to measure, estimate or predict, and that could adequately predict evaporation in a more efficient way than its complex measurement. To do so, we combined physical lake modelling and climate reanalysis into a multi-model approach to estimate evaporation from 187 reservoirs across the globe. More precisely, we analyzed the relations between annual evaporation and (1) depth, (2) surface area, and (3) thermocline depth (Z_{therm}). We think the results of such analysis can contribute to better water resource management and provide indications on ways to design reservoirs with reduced evaporative water losses and water footprints.

2.2 METHODS

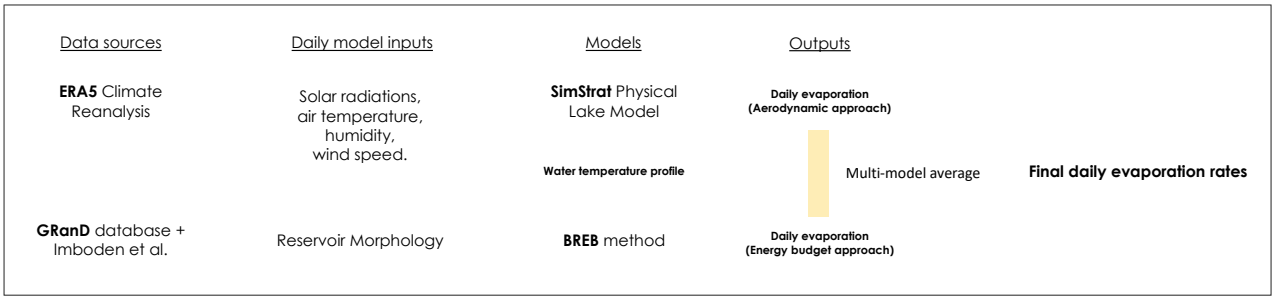

Figure 2.1 Visual representation of the workflow used to estimate evaporation from the 187 reservoirs across the globe. Meteorological data and morphology needed to input in evaporation equations and physical lake modeling were obtained from global databases, idealized morphology estimation equations (Imboden et al., 1973) and climate reanalysis. Evaporation was estimated at the daily time scale, with two different equations. The equally weighted average of both daily rates was subsequently summed to an annual rate for each individual reservoir.

2.2.1 Reservoirs and period selection

Reservoirs were randomly selected based on the availability of their characteristics in the Global Reservoir and Dam Database (GRanD) v1.3 (Lehner et al. 2011). This database is a cumulation of different datasets and is managed by McGill University (Montreal, QC, Canada). In total, 187 different reservoirs were selected across the 4 main Köppen-Geiger climates (figure 2.2), with a variety of morphometric characteristics and physical properties (table 2.1). Dispersing the reservoirs across different climates ensured the inclusion of a variety of weather conditions (table 2.2). The modelling period was arbitrarily selected as the year 2017, to include reservoirs of different ages.

Table 2.1 Summary statistics of morphology and physical properties of the 187 reservoirs used in this study.

Morphology	Units	Min.	Mean ± SD	Median	Max.
Surface area	(km^2)	0.09	126.1 ± 540.0	7.8	5277
Volume	(million m^3)	1	4035 ± 18963	141	185000
Maximum depth	(m)	8	54 ± 43	42	243
Average depth	(m)	3	22 ± 19	15	110
Surface area to volume ratio	(m^{-1})	0.01	0.07 ± 0.05	0.07	0.29
Physical properties					
Average thermocline depth	(m)	1.8	4.9 ± 2.7	4.5	12.9
Number of days with stratification	(days)	1	232 ± 95	248	365

Note: Average thermocline depth was calculated as the average of daily depths and the days of stratification are the number of days without a thermocline.

Table 2.2 Summary statistics of weather conditions over the 187 reservoirs used in this study. The weather variables are the average of daily values over the year of 2017, from ERA5 climate reanalysis.

Weather variables	Units	Min.	Mean ± SD	Median	Max.
Air temperature	(°C)	-2.7	16.1 ± 8.4	18.0	29.3
Water surface temperature	(°C)	4.8	21.3 ± 8.1	23.2	32.5
Incoming shortwave radiations	(MJ m^{-2})	7.2	15.9 ± 3.8	16.6	22.7
Vapor pressure of air	(kPa)	0.49	1.49 ± 0.62	1.47	2.91
Wind speed	(m s^{-1})	0.2	1.8 ± 0.7	1.8	4.1

2.2.2 Estimation of annual evaporation

Daily evaporation was estimated as the equally weighted average of the rates obtained from two different estimation equations, i.e., the Bowen Ratio Energy Budget and the mass transfer methods. This approach showed itself to be accurate when compared against measured evaporation rates by eddy covariance from two different reservoirs in contrasting climates (Chapter 1). Daily rates were subsequently summed to obtain an annual estimate for each reservoir.

2.2.2.1 Bowen Ratio Energy Budget method

The Bowen Ratio Energy Budget (BREB) method is based on the conservation of energy laws. It accounts for incoming, outgoing, and stored energy in a system. It can be expressed as follow (Lenters et al. 2005):

$$N = R_n + A_n + G_n - H - L,$$

where N is heat storage of the water body, R_n is net radiations at the water surface, A_n is net advected energy, G_n is net energy exchange between the sediments and overlying water, H is sensible heat flux and L is latent heat flux. By rearranging this equation, evaporation (E) can be derived from latent heat (L) and water's latent heat of vaporization (λ):

$$L = \lambda E,$$

$$E = \frac{R_n + A_n + G_n - H - N}{\lambda}.$$

The sensible heat flux term cannot be determined readily unless there are instruments in place to perform direct measurements. Bowen (1926) developed a method to describe the ratio of sensible to latent heat, termed the Bowen ratio (β). A modified form to obtain β without direct measurement of sensible heat was developed (Brutsaert 2013):

$$\beta = \frac{H}{L} = \frac{c_p \emptyset (T_s - T_a)}{\varepsilon_m \lambda (e_s^* - e_a)},$$

where c_p is the specific heat of air at constant pressure, $\emptyset$ is the atmospheric pressure, T_s and T_a are the temperatures of the water surface and the air, ε_m is the ratio of molecular weight of water to that of dry air, e^*_s is saturation vapour pressure at water surface temperature and e_a is the vapour pressure of the overlying air. The ratio $c_p \emptyset / \varepsilon_m \lambda$ is also termed the psychrometric constant, γ. By substitution, we can eliminate the sensible heat term in the first equation and obtain the following, which constitutes the BREB method:

$$E = \frac{R_n + A_n + G_n - N}{\lambda(1 + \beta)}.$$

The exchange of energy in a water body is usually governed by exchanges at the water surface and heat storage in deep lakes (stratified), rather than advected energy and sediment conduction (Henderson-sellers, 1986). For shallow lakes, sediment conduction can however be significant (Sturrock et al. 1992). Thus, the final equation was simplified to the following, termed reduced energy budget (Finch and Calver, 2006):

$$E = \frac{R_n + G_n - N}{\lambda(1 + \beta)}.$$

Details of the computation of individual energy budget components are available in supplemental materials (appendix D).

Daily evaporation rates estimated by the BREB method were inspected and modified to meet certain quality criteria. Evaporation values are problematic when the Bowen ratio (β) is close to -1 (Irmak et al. 2014). This is clear from the formulation of the last equation, where a β close to -1 would cause an inaccurately large evaporation value. This usually happens in pseudo-adiabatic conditions, where the saturation mixing ratio is close to the specific humidity of the air (Savage et al. 2009). Therefore, evaporation rates were rejected when β was between -1.3 and -0.7, as recommended by Kurc & Small (2004). Similarly, when the vapour pressure deficit is close to zero, the resulting β is inaccurately high, causing uncertainty in evaporation estimation. Thus, data was rejected when the vapour pressure deficit was between -0.05 and 0.05. Evaporation values on the first day of every reservoir simulation were also rejected, because of the way heat storage (*N*) is estimated. Because it relies on water temperature values from the prior day, it was impossible to estimate it and evaporation would be biased as a result.

2.2.2.2 Mass transfer

The mass transfer method used in this study is an integrant part of the Simstrat physical lake model. It estimates free-water evaporation with an equation based on Dalton's law (Dalton, 1802), which relates evaporation to wind speed and the vapour pressure deficit between the water surface and the atmosphere. It takes the form of:

$$E = f(u)(e_s^* - e_a),$$

where *f(u)* is a wind function describing the drying power of air, e^*_s is saturation vapour pressure at water surface temperature and e_a is the vapour pressure of the overlying air. The wind function used is the Ryan-Harleman equation (Ryan et al., 1974), with modifications proposed by Adams et al. (1990):

$$f(u) = \sqrt{(2.7\Delta\theta^{1/3})^2 + (3.1U)^2},$$

where $\Delta\theta$ is a term accounting for the increase in driving buoyancy force by evaporation and U is wind speed. This equation gives more weight to the second term, i.e., forced convection (wind-driven) than the first term, free convection (buoyancy driven) in the process of evaporation. It is advantageous in the context of modelled water temperature since errors in modelled temperature will have less effect on evaporation rates. When ice cover is expected, the equations are switched. Simstrat simulates lake ice

formation and decay according to Leppäranta (2010, 2014) and Saloranta and Andersen (2007), which propose to use a variation of the mass transfer equation, i.e., a bulk transfer equation. The bulk transfer formula is expressed as:

$$E = k_c U(q_s - q_a),$$

where k_c is the bulk exchange coefficient, U is wind speed, q_s is specific humidity at the water surface temperature, q_a is specific humidity of the air. The bulk exchange coefficient is constant at 1.5 x 10^{-3} according to recommendations made by Leppäranta (2010). For more details regarding the different equations, parameters and their computation, readers are referred to Simstrat's documentation (available freely on "Eawag – Applied System Analysis" GitHub), Goudsmit et al. (2002) and Schmid and Köster (2016). For the ice module specifically, see Gaudard et al. (2019).

2.2.2.3 Additional data processing

Daily rates estimated by both methods were modified as follows. Negative evaporation values represent conditions where condensation is occurring. Because we are interested exclusively in evaporation, these were converted to null. Data was also converted to null when ice cover was predicted by Simstrat internal ice module. Sublimation does happen but was deemed negligible because the energy required for it to happen is higher than for evaporation and the albedo of ice is much higher than water (more than 10 times higher on average). An albedo of this magnitude means that most of the energy from solar radiation is reflected to the atmosphere (Wang et al. 2018).

2.2.3 Water temperature profile modelling

Water temperature profiles are necessary for the computation of evaporation estimation equations. Consequently, physical lake modelling was used to estimate daily water temperature profiles. We used the Simstrat 1D physical lake model, a one-dimensional physical lake model for the simulation of deep lake stratification and mixing developed at the Swiss Federal Institute of Aquatic Science and Technology (Eawag), in Switzerland. It uses a k-ε energy closure scheme for turbulent mixing and includes internal energy transfer via internal seiches (Goudsmit et al. 2002). Its accuracy was demonstrated on multiple water bodies in different settings (Gaudard et al., 2017, 2019) and is regularly reviewed and updated. The model was executed through R Studio (R core team 2021) with the "LakeEnsemblR" library (Moore et al. 2021).

To simulate a temperature profile, Simstrat requires a minimum of water body bathymetry, meteorological data (wind speed, humidity or dewpoint temperature, air temperature, atmospheric pressure, incoming solar radiations) and light extinction coefficient (k_d). More data can also be included for increased accuracy (see Moore et al. 2021). All meteorological inputs were obtained from the climate reanalysis tool ERA5. We chose to set the extinction coefficient to an arbitrary value of 1.0 m^{-1}. This choice had an inevitable effet on thermocline depth estimation, but we deemed it acceptable siunce we were interested in broad patterns rather than absolute relationships. Additionnaly, its value was not available for each individual reservoir. Water and ice albedo was set to constant values of 0.08 and 0.9, respectively. Simstrat requires the input of the fraction of seiche energy to total wind energy, which was set at a constant value of 0.01 as proposed by Simstrat's documentation as a typical value. A wind sheltering component was included to account for the effect of fetch on energy transfer from wind to the lake surface, which was modeled as follow, according to Hondzo and Stefan (1993):

$$W_{str} = 1 - \exp\left(-0.3 \times A_s\right),$$

Where A_s is surface area in km^2. Hypsography of each reservoir was estimated according to Imboden (1973), with details available in appendix C. Surface area and maximum depth were taken from GRanD and average depth was taken as the ratio of total volume to surface area.

2.2.4 Thermocline depth estimation

We defined the thermocline as the depth of maximum density gradient, with a threshold gradient of 0.1 kg/m^3 at a vertical resolution of 0.1 meters. We calculated its depth daily before averaging it over a year. Days without stratification were not included it the averaging.

2.2.5 Climate reanalysis

Climate reanalysis from ERA5 (Copernicus Climate Change Service, 2017) was used to provide meteorological inputs needed in the computation of evaporation estimation equations and the modelling of water temperature. ERA5 is the fifth-generation atmospheric reanalysis of global climate by the European Centre for Medium-range Weather Forecast (ECMWF). It provides hourly estimates of numbers of climatic variables, covering Earth on a horizontal $30km^2$ grid on 137 levels of vertical resolution, up to a height of 80km. Data is available from 1979 onwards, within 3 months of real-time. ERA5 combines observational data, advanced modelling, and data assimilation systems to provide climate reanalysis

datasets (Hersbach et al., 2020). The reanalysis dataset "ERA5-Land hourly data from 1981 to present" was used for the present study. It was produced through models driven by near-surface atmospheric fields from ERA5, with thermodynamical orographic adjustment of temperature and lapse-rate correction of other components (Muñoz-Sabater, 2019). These modifications to the ERA5 basic dataset added the benefit of an increased spatial resolution of 9km^2. Details of the reanalysis variables used for this study are available in supplemental materials (appendix A).

2.2.6 Statistical analysis

Generalized additive models (GAM) were used to detect and describe the relationships between morphometric characteristics (mean depth, maximum depth, surface area), Z_{therm} and annual evaporation. We used the GAM with a gaussian family distribution and restricted maximum likelihood (REML) fitting method in all cases. Model validity was assessed from basis dimension check, residuals and partial residual plots, as well as probability plots (Q-Q plots). The duration of stratification (in days) was added to the predictive model with Z_{therm} because we hypothesized that reservoirs with similar Z_{therm} but stratified for different lengths of time would not have the same annual evaporation rate. We used Pearson correlation to check for co-linearity between these two variables before doing so.

All data processing and statistical analysis were performed with R studio (R Core Team 2021). A list of used libraries with corresponding authors is included in supplemental materials (appendix E).

2.3 RESULTS

Annual evaporation estimates varied between 152 and 1792 mm, with an average of 927 and a standard deviation of 362 mm. Average evaporation was highest in the arid climate (1281 mm) followed closely by the tropical climate (1240 mm). The lowest average rates were in the continental climate (mean of 450 mm). Average evaporation in the temperate climate was almost twice as high as in the continental climate (897 mm). Evaporation rates represented on average 6.4% of reservoir's inflow, with values starting near 0% and going as high as 49%.

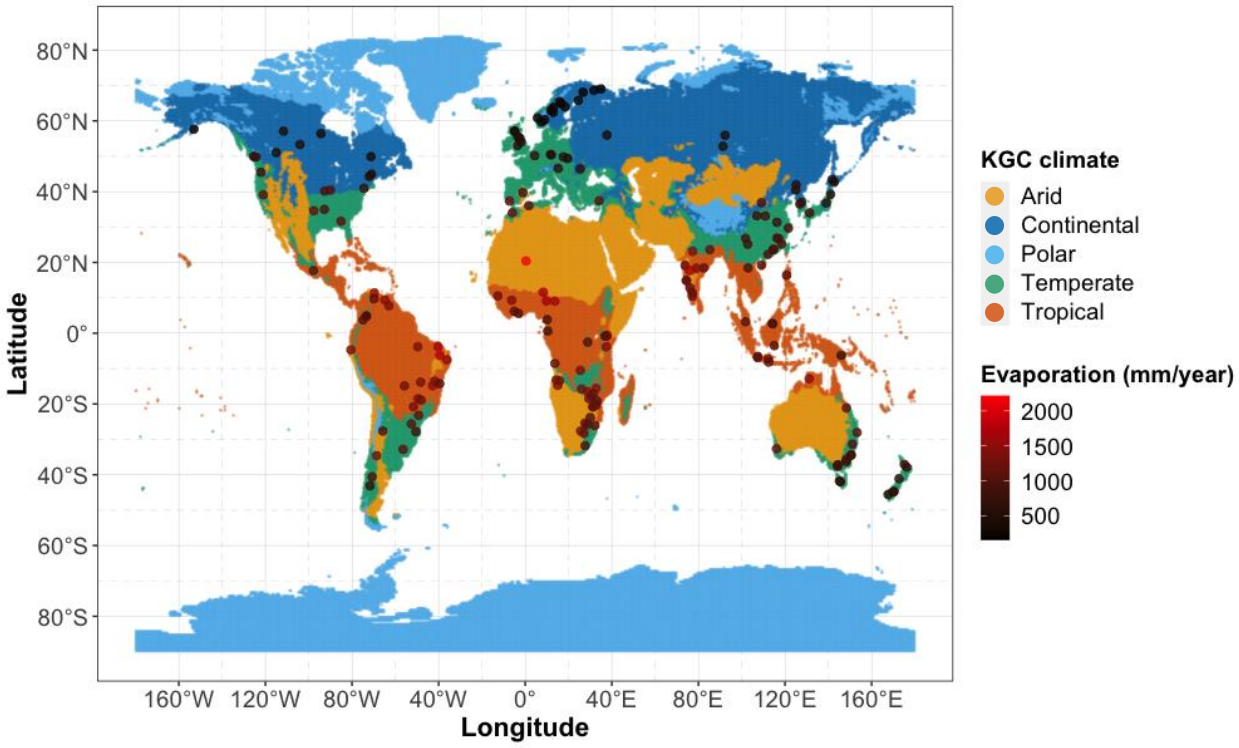

Figure 2.2 Estimated annual evaporation rates of 187 reservoirs across the globe, in different climates. The circles represent the individual reservoirs with their color representing the magnitude of their evaporation rate. Map colors represents the 5 main climates denomination as per the Köppen-Geiger Climate Classification scheme.

Predicting annual evaporation with average thermocline depth (Z_{therm})and duration of stratification explained 76% of the deviance in the model, with an R^2 of 77%. The partial effect of Z_{therm} on annual evaporation was highest and followed a logarithmic relationship, rising linearly from 2 to 6 meters and reaching a plateau afterwards (figure 2.3a). In other words, the model predicts the shallower the average Z_{therm} of a reservoir is, the lower its annual evaporation rate, up to a depth of 6 meters. Evaporation is then constant at its maximum for deeper Z_{therm}. The duration of stratification had a nonlinear relationship with the response variable, such that the number of days had a negative relationship with annual evaporation up to a duration of 140 days, and a constant relationship with longer durations (figure 2.3b). No significant relationships were detected between any of the morphometric characteristics we related with reservoir annual evaporation, i.e., surface area, mean depth, and maximum depth. Results of attempted models are available in supplemental materials (appendix F).

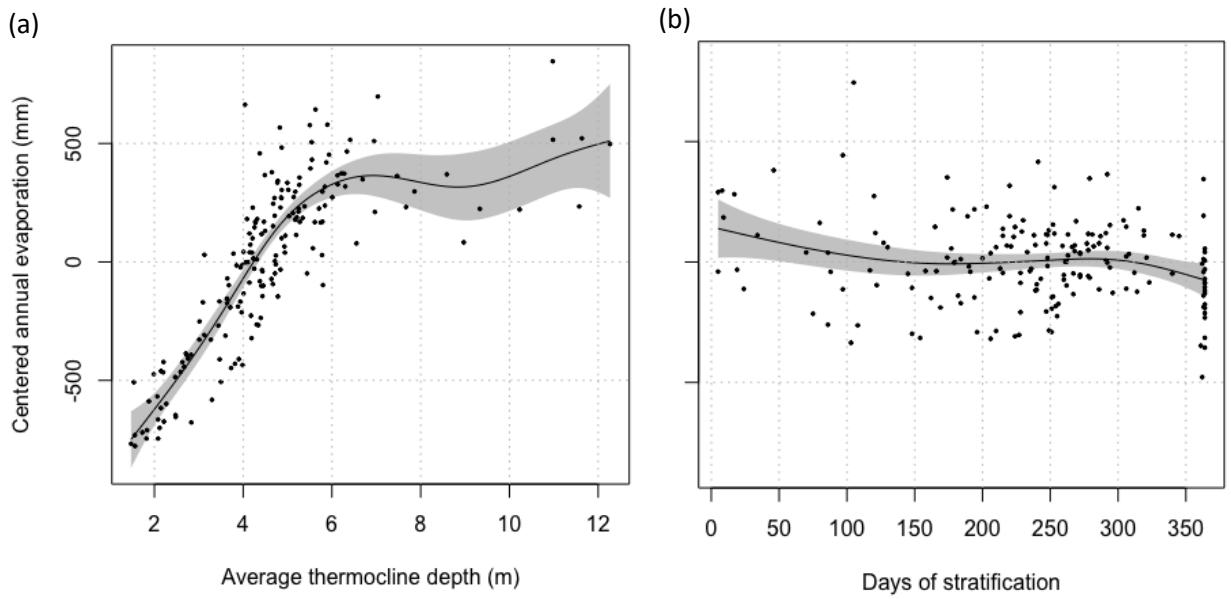

Figure 2.3 Generalized linear model (GAM) showing the partial effects of (a) average thermocline depth and (b) number of days of stratification on annual evaporation from reservoirs. Dots are the partial residuals of the model and shaded areas represent the 95% confidence intervals. The y-axis is centered evaporation around the mean of the dataset (914 mm). Average thermocline depth was calculated as the average of daily depths and the days of stratification are the number of days without a thermocline. (*n = 187*)

2.4 DISCUSSION

2.4.1 Relationships with morphology

According to the energy budget view of evaporation, available energy plays a important role in the evaporation process (Finch and Calver, 2008). Most energy stored in a water body comes from solar radiations, which are area dependent. Therefore, we expected that for reservoirs with the same volume, higher surface area would lead to more absorbed energy, and to more available energy per m^3 of water. If correct, we should have observed relationships between morphological traits of reservoirs and evaporation, especially with mean depth, i.e. the ratio between volume and surface area. There were however no relationships with any of them (appendix F). The majority of reservoirs in our dataset were stratified at some point during the year (180 out 187 reservoirs). During stratification, the dense water of the hypolimnion becomes sheltered from surface processes like wind mixing and solar radiations (Monismith and MacIntyre, 2009). The incoming energy is mostly transferred to the water in the upper portion of the reservoirs, over the thermocline (the epilimnion). This could explain the lack of relationships between basic morphology and evaporation and support the relationships from both Z_{therm} and the duration of stratification with evaporation.

2.4.2 Relationship with thermocline depth

Since surface heating from solar radiations and warm air tend to promote stronger stratification and shallower surface mixed layer (SML), we can expect reservoirs with deep thermoclines to have thes coldest surface temperatures (Wüest and Lorke, 2003). A larger volume of water in the SML exposed to the same radiations should have less energy per m^3, thus less energy available to warm the water column. This would result in lowered surface water temperature and reduced temperature difference between the air and the water surface (Wang et al., 2018). Ultimately, it would reduce energy losses by sensible and radiant (longwave radiations) heat and leave more available energy for evaporation (Brutsaert, 1982). Concurrently, lowered air-water temperature difference should lead to lower vapour pressure deficit (VPD) between the water surface and the atmosphere. In turn, physics relates lower VPD with lower diffusion of water vapour (Dingman, 2015). Lower water temperature thus has contrasting effects on evaporation through its effect on different components, but our results shows a positive relationship between evaporation and Z_{therm} (figure 2.3a) This suggest that the effect of the air-water temperature gradient on evaporation outweights the effect of VPD. This could be explained by the fact that even with reduced VPD, water molecules can still be diffused by other processes if they have enough energy to change phase.

Wind is arguably the biggest driver of thermocline depth, which could also help to explain our results. Turbulence introduced by wind in the water column during mixing events fights against surface heating from solar radiations to prevent stratification (Wüest and Lorke, 2003). Once a water body is stratified, this turbulence favors entrainment of deeper, denser water from below the thermocline into the SML, thus deepening the thermocline (Spigel and Imberger, 1980). Wind can also have an effect on evaporation. Diffusion of water vapor from the water surface to the atmosphere is proportional to the VPD between air and water (Dingman, 2015). Wind has the ability to mix the water vapor directly above a water body with its overlying air, thus decreasing local humidity at the air-water interface. As a result, VPD immediately over the water surface would increase, enhancing evaporation at the same time (McVicar et al., 2012). This could also explain why we observed a rising trend between thermocline depth and evaporation even if we expected a lower VPD from a reduced surface water temperature. All in all, the simultaneous effect of wind on both Z_{therm} and evaporation supports the relationship we observed between Z_{therm} and evaporation (figure 2.3a).

An interesting reflexion is that evaporation has an effect on water surface temperature. Water needs energy to change phases during the process of evaporation. This consumption of energy results in

the cooling of surface water, a process called evaporative cooling (Dake, 1972). Cooled surface water sinks because of density changes. This free convection introduces turbulent kinetic energy in the SML and weakens buoyancy and stability in the water column, which could favor the deepening of the thermocline or its acceleration (Monismith and MacIntyre, 2009). Higher evaporation rates could indirectly be linked to deeper thermoclines in this way. Nonetheless, evaporative cooling certainly contributes to a lower surface temperature, helping in the reduction of heat losses in the form of radiant and sensible heat.

We can use SML dynamics to investigate the stable horizontal relationship between evaporation and Z_{therm} deeper than 6 meters (figure 2.3a). The total energy required to produce sufficient turbulence in the SML to deepen the thermocline increases as its volume rises. Energy input from the surface might not be enough at this point to drive SML deepening. There is also a complex interaction between thermocline deepening caused by mechanical forces and convection, with the former increasing stability and the other, decreasing it. That is because mechanical forcing does not change buoyancy forces while convection decreases them (Wüest and Lorke, 2003). Thus, we could assume that in reservoirs with high stability, the depth of the thermocline is determined mostly by mechanical energy from wind and shear. Since wind is generally assumed to be the biggest driver of thermocline formation, we can presume that the deepest thermoclines, over 6 meters in our case, suggest overall more stable SMLs.

Limitations in our methods need to be considered when interpreting the relationship from figure 2.3a. The definition of thermocline depth varies in the literature (Fiedler, 2010). In our study, we defined it as the depth of maximum density gradient at a resolution of 0.1 meters, which we calculated daily before averaging it over a year. This method of estimation does not discriminate diurnal from seasonal thermocline. There is a possibility that this brought errors in our estimation of Z_{therm}. We also used the same light extinction coefficient (k_d) for every reservoir, which showed itself to impact significantly on the depth of thermocline (unpublished results, see chapter 1 and appendix B). This would most likely not change the relationship between thermocline and annual evaporation. However, the different values of evaporation and Z_{therm} should not be taken as absolute values until further investigation of the effect of a constant k_d on the relationship.

2.4.3 Relationship with the duration of stratification

Figure 2.3b shows the relationship between annual evaporation and the duration of stratification, assuming a Z_{therm} of 4.7 meters (the mean of the dataset). We can conclude from this figure that for the

same average Z_{therm}, reservoirs with the shortest duration of stratification have the highest annual evaporation rates, up to a duration of approximately 160 days. For longer durations, there are no predicted differences in evaporation. With Z_{therm} positive effect on evaporation, we would have expected that a longer period with a thermocline would result in higher evaporation. The fact that the thermocline tends to deepen throughout a reservoir stratification period reinforced that expectation. The absence of stratification on a given day could be attributed to either low stability or high turbulence (Boehrer and Schultze, 2009; Wüest and Lorke, 2009). Evaporation generates turbulent kinetic energy by free convection of cooled water from the surface. It also suppresses stability by reducing the density gradient between the epilimnion and the hypolimnion. As a result, mixing is accelerated (Wüest and Lorke, 2003; Monismith and MacIntyre, 2009). This suggests that higher annual evaporation might be linked to reduced durations of stratification, as observed in this study (figure 2.3b). However, this leads to two contrasting interpretations when downscaling the process at a daily timescale. On one hand, daily evaporation on stratified days could be lower than on mixed days, summing up to higher annual evaporation with shorter durations of stratification. On the other hand, it could be that daily rates caused by the presence of a thermocline on stratified days (as suggested by figure 2.3a) are high enough to compensate for the lower rates of mixed days. If we consider 2 different reservoirs with the same average Z_{therm} but with different duration of stratification, the reservoirs with the lowest duration would have deeper daily Z_{therm}. This would support the latter explanation, as we expect from our results that deeper thermoclines are linked with higher evaporation rates. Further analysis at the daily timescale would be needed to address this and to better understand the relationships found in our study.

2.5 CONCLUSION

The objective of this study was to relate the annual evaporation of reservoirs with their morphology and physical properties and find indicators that would allow us to predict evaporation in a more efficient way than its complex measurement. We did so by combining physical lake modelling and climate reanalysis into a multi-model approach to estimate evaporation from 187 reservoirs across the globe. While no relationships were found between morphology and annual evaporation, it led us to narrow our analysis to the surface mixed layer, in which most of the incoming energy is transferred, generated, and consumed. Although opposite to what we hypothesized, we found a relationship between annual evaporation and the combination of thermocline depth and duration of stratification as expected. Annual evaporation was lowest with lower thermoclines, rising linearly from 2 to 6 meters, where evaporation is at its highest and constant for deeper thermoclines (figure 2.3a). We gave several explanations that might explain this

relationship. Reduced heat losses from lowered temperature differences between the water surface and the atmosphere expected from a lower thermocline might provide more energy for evaporation. When looking at the relationship the opposite way, we argued that high evaporation rates suggested more turbulence and less stability, both leading to deeper thermoclines. For thermoclines deeper than 6 meters, energy inputs by evaporation might not be enough to deepen the SML, and complex interactions between mechanical and convection forces could have increased stability, resulting in the observed constant relationship. Annual evaporation was highest with short durations of stratification from 1 day up to 160 days and stabilized at its lowest for longer durations (figure 2.3b). Reduced stability and density gradient caused by high evaporation rates were suggested as an explanation for this relationship. We proposed in both cases that downscaling our analysis to a daily timescale might help in supporting our results and conclusions.

To conclude, we suggest that thermocline depth and duration of stratification constitute a good proxy for predicting evaporation from reservoirs since they are determined and influenced by mostly the same variables (solar radiations, wind, temperature, other mechanical sources of energy like shear or seiches, etc.). It is also much easier to measure or predict than actual evaporation, offering an alternative to complex, time-consuming logistics. This study represents a first attempt at upscaling reservoir evaporation to the global scale and a springboard to multiple possibilities. We believe that our results can be used to improve water resource management and provide indications on ways to design reservoirs with reduced evaporative water losses and water footprints.

CONCLUSION DU MÉMOIRE

L'évaporation des lacs et des réservoirs constitue une importante perte d'eau douce partout dans le monde. C'est pourquoi ce mémoire soutient qu'il est important d'avoir l'habilité de l'estimer de manière efficace à l'échelle globale. La littérature est saturée de méthodes d'estimation différentes, mais aucune d'entre-elle ne s'est avérée applicable dans toute situation. Notre compréhension du phénomène de l'évaporation est conséquemment incomplète. Cette étude avait pour but de contribuer à cette problématique.

Cette contribution s'évalue de différentes façons. D'abord, le premier chapitre a constitué une étape vers une méthodologie universelle pour estimer l'évaporation journalière de surface d'eau libres qui réduit grandement les défis associés à sa mesure directe. Cette méthode consistant en la combinaison de données de réanalyse météorologique et de la modélisation physique de la température de l'eau s'est avérée efficace. L'évaporation journalière provenant de deux réservoirs différents ont été reproduites avec une bonne précision, sans la nécessité de mesurer la météo *in situ,* une exigence de la majorité des méthodes proposées jusqu'à ce jour. Une meilleure précision est possible en mesurant les données les plus sensibles, notamment les radiations solaires et la vitesse du vent, mais ne se sont pas avérer nécessaire pour une précision acceptable. Nous attribuons ce succès à la combinaison d'une approche aérodynamique avec une approche de bilan énergétique. Ce résultat est important puisque cette méthode est applicable dans la majorité des situations, pour estimer l'évaporation à part entière ou bien encore pour compléter des données manquantes dans un plus grand jeu de donnée. Cette méthode pourrait être utile pour déterminer l'évaporation d'étendues d'eau éloignés, difficile à atteindre ou sans stations météorologiques, ou encore pour prédire celle de futurs réservoirs. Nos résultats suggèrent la validité de cette méthode pour effectuer des analyses à plus grande échelle, ce qui n'était pas facilement réalisable jusqu'à maintenant. Une analyse de ce type a donc été effectuée dans le chapitre 2. En modélisant l'évaporation de 187 réservoirs partout dans le monde *avec la même méthodologie*, nous avons été en mesure d'analyser les relations entre leur taux d'évaporation annuel et différentes caractéristiques. Notamment, une relation importante avec la profondeur moyenne de la thermocline et la durée de stratification a été identifiée. L'évaporation annuelle augmente avec cette profondeur, de 2 jusqu'à 6 mètres, et se stabilise à son maximum pour toute profondeur plus grande. En relation avec la durée de stratification, l'évaporation annuelle diminue d'une durée de 1 jusqu'à 160 jours, puis se stabilise à son minimum pour les durées plus longues. D'un point de vue pratique, ce résultat nous permet

potentiellement de déterminer ou encore de prédire l'évaporation annuelle d'un réservoir par la mesure ou la prédiction de la profondeur de sa thermocline et la durée de stratification, deux paramètres plus faciles à mesurer et à prédire que l'évaporation directe. Il nous permet aussi d'améliorer notre capacité de gestion de ressources hydriques en appuyant la conception de réservoirs à perte d'eau et empreinte eau réduite, ou en optimisant la gestion du niveau de l'eau et de la génération hydroélectrique.

À notre connaissance, cette étude est la première à proposer une méthode d'estimation universelle et la première étude à grande échelle de l'évaporation annuelle d'étendues d'eau. Les résultats obtenus représentent d'importantes contributions scientifiques et pourraient servir de tremplin pour de futures études adressant des problématiques modernes. Notamment, la combinaison de cette approche avec une méthode d'estimation d'évapotranspiration du paysage pré-inondation pourrait permettre la détermination de l'empreinte eau des réservoirs. Ces empreintes pourraient ensuite être mises en relation avec par exemple, des caractéristiques du paysage tel que le type de végétation, leur couverture totale, la topographie, la géologie et la pédologie locale, ou encore avec les mêmes caractéristiques présentées dans cette étude. Des comparaisons entre empreinte eau et évaporation pourraient alors être effectuées. De plus, la possibilité de varier le coefficient d'extinction lumineuse dans notre approche de modélisation pourrait servir de plateforme pour décrire les changements d'évaporation en fonction de différents niveaux d'eutrophisation.

APPENDIX A

Description of variables from ERA5 climate reanalysis dataset used in this study

Table A1 List and details of ERA5 variables used in this study, with ECMWF official description and their use in this study. Variables are from "ERA5-Land hourly data from 1981 to present" reanalysis dataset.

Variable	Units	Description (Copernicus Climate Change Service 2017)	Use in this study
10m u-component of wind	$m\ s^{-1}$	Eastward component of the 10m wind, at a height of ten metres above the surface of the Earth.	Simstrat forcing variable.
10m v-component of wind	$m\ s^{-1}$	Northward component of the 10m wind, at a height of ten metres above the surface of the Earth.	Simstrat forcing variable.
2m dewpoint temperature	°K	Temperature to which the air, at 2 metres above the surface of the Earth, would have to be cooled for saturation to occur. It is calculated by interpolating between the lowest model level and the Earth's surface, taking account of the atmospheric conditions.	Simstrat forcing variable; vapor pressure of air.
2m temperature	°K	Temperature of air at 2m above the surface of land, sea or in-land waters. 2m temperature is calculated by interpolating between the lowest model level and the Earth's surface, taking account of the atmospheric conditions.	Simstrat forcing variable; Bowen Ratio calculation.
Surface pressure	Pa	Pressure (force per unit area) of the atmosphere on the surface of land, sea and in-land water.	Simstrat forcing variable; Bowen Ratio calculation.
Surface solar radiation downwards	$J\ m^{-2}$	Amount of solar radiation (also known as shortwave radiation) reaching the surface of the Earth. Comprises both direct and diffuse solar radiation. Radiation from the Sun (solar, or shortwave, radiation) is partly reflected to space by clouds and particles in the atmosphere (aerosols) and some of it is absorbed. The rest is incident on the Earth's surface (represented by this variable). To a reasonably good approximation, this variable is the model equivalent of what would be measured by a pyranometer (an instrument used for measuring solar radiation) at the surface.	Simstrat forcing variable; net radiation term for evaporation.
Surface thermal radiation downwards	$J\ m^{-2}$	Amount of thermal radiation (also known as longwave or terrestrial) emitted by the atmosphere and clouds that reaches the Earth's surface. The surface of the Earth emits thermal radiation, some of which is absorbed by the atmosphere and clouds. The atmosphere and clouds likewise emit thermal radiation in all directions, some of which reaches the surface (represented by this variable).	Simstrat forcing variable; Net radiation term for evaporation.

APPENDIX B

Modeled water temperature profiles by Simstrat 1-D physical lake model

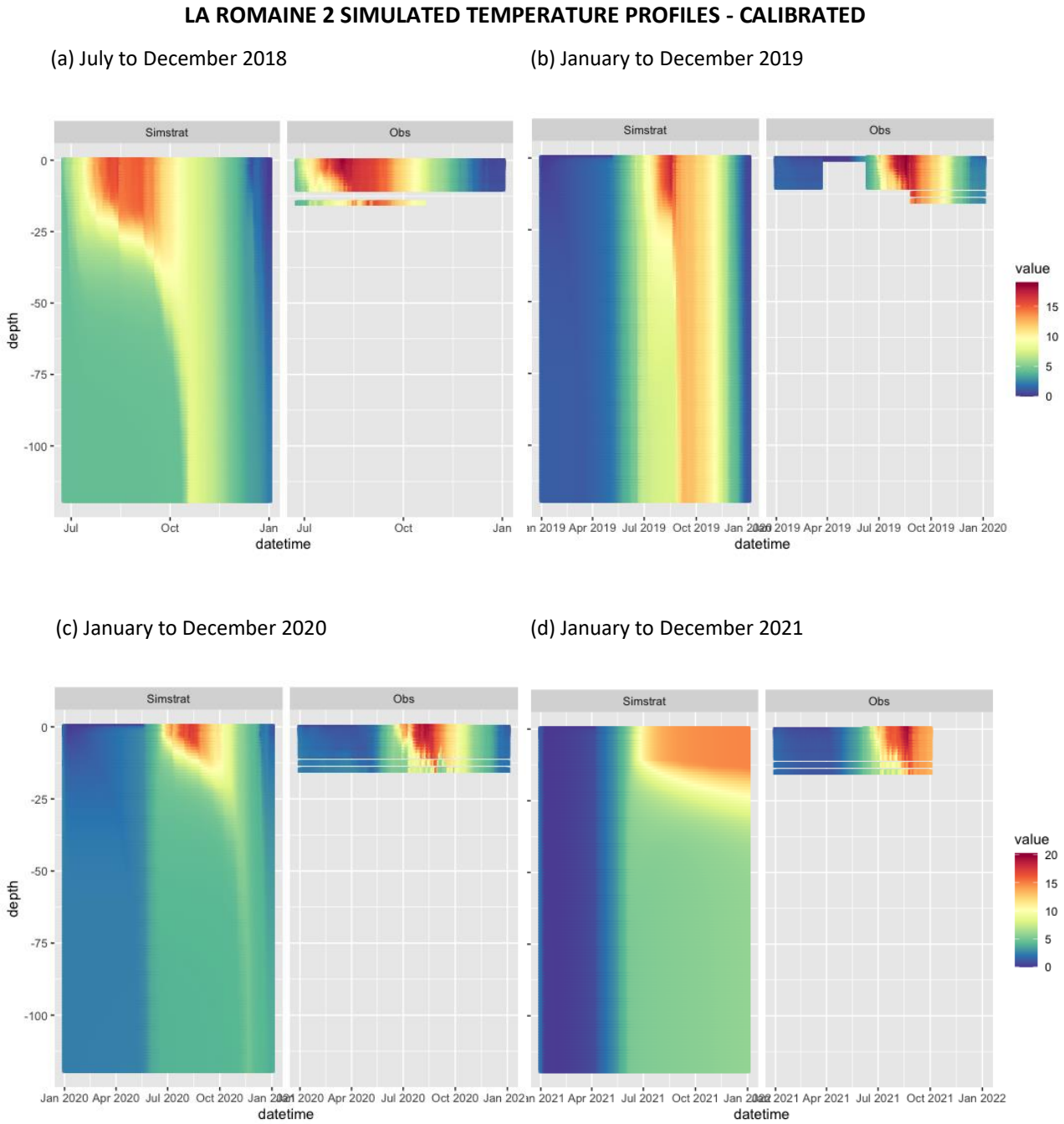

Figure B1. Simulated temperature profiles at La Romaine 2, by Simstrat physical lake model with Latin Hypercube calibrated a_{seiche} parameter and mean annual observed k_d (0.5 m^{-1}). Figures labeled “Simstrat” are simulated profiles and “obs” are the measured available thermal surveys.

LA ROMAINE 2 SIMULATED TEMPERATURE PROFILES - UNCALIBRATED

(a) July to December 2018 (b) January to December 2019

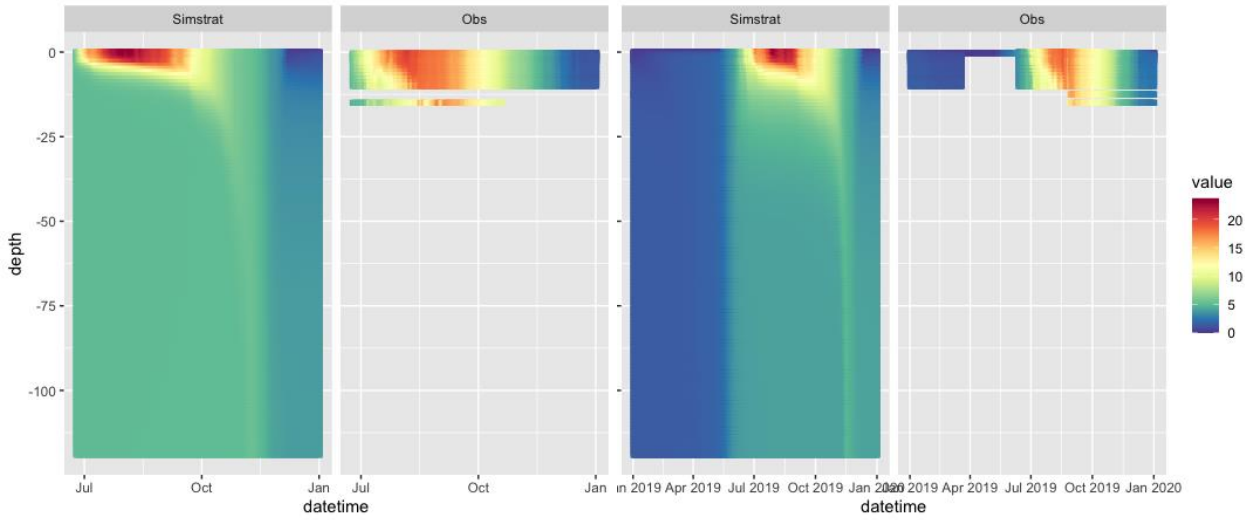

(c) January to December 2020 (d) January to December 2021

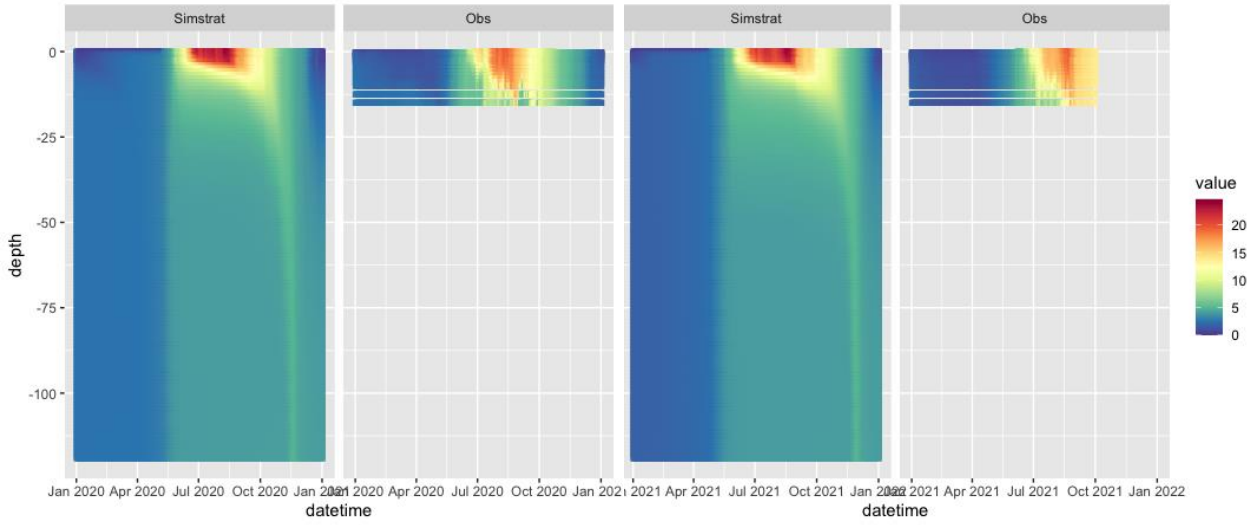

Figure B2. Simulated temperature profiles at La Romaine 2, by Simstrat physical lake model without calibration of the a_{seiche} parameter and an arbitrary k_d of 1.0 m^{-1}. Figures labeled “Simstrat” are simulated profiles and “obs” are the measured available thermal surveys.

NAM THEUN 2 SIMULATED TEMPERATURE PROFILES - CALIBRATED

(a) January to December 2009 (b) January to December 2010

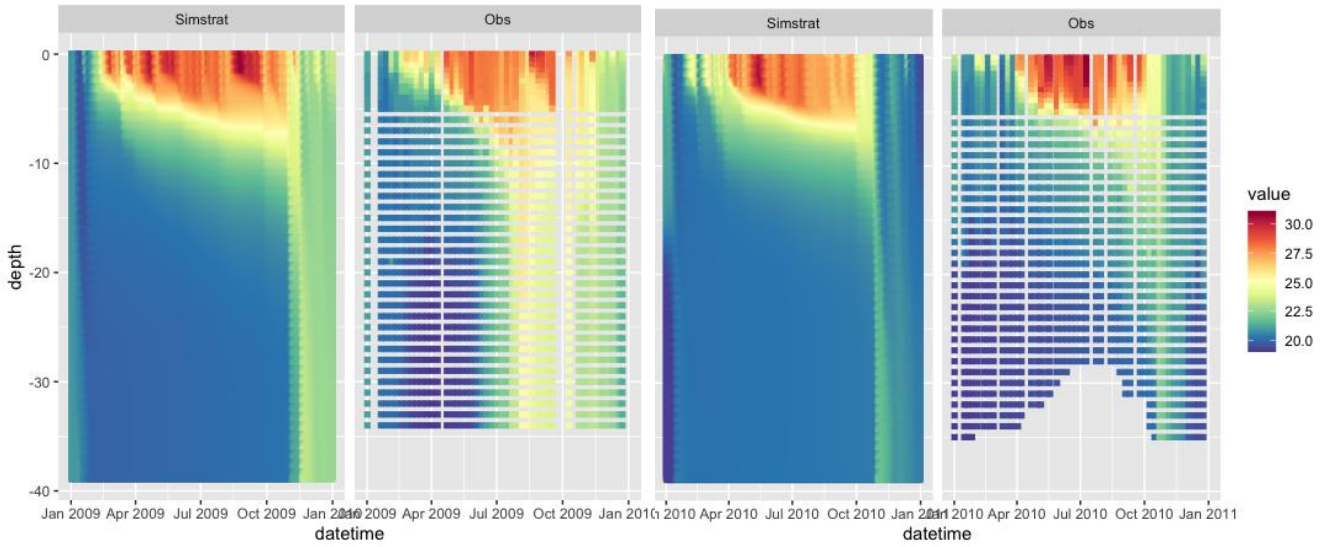

Figure B3 Simulated temperature profiles at Nam Theun 2, by Simstrat physical lake model with Latin Hypercube calibrated a_{seiche} parameter and mean annual observed k_d (0.7 m^{-1}). Figures labeled "Simstrat" are simulated profiles and "obs" are the measured available thermal surveys.

NAM THEUN 2 SIMULATED TEMPERATURE PROFILES - UNCALIBRATED

(a) January to December 2009 (b) January to December 2010

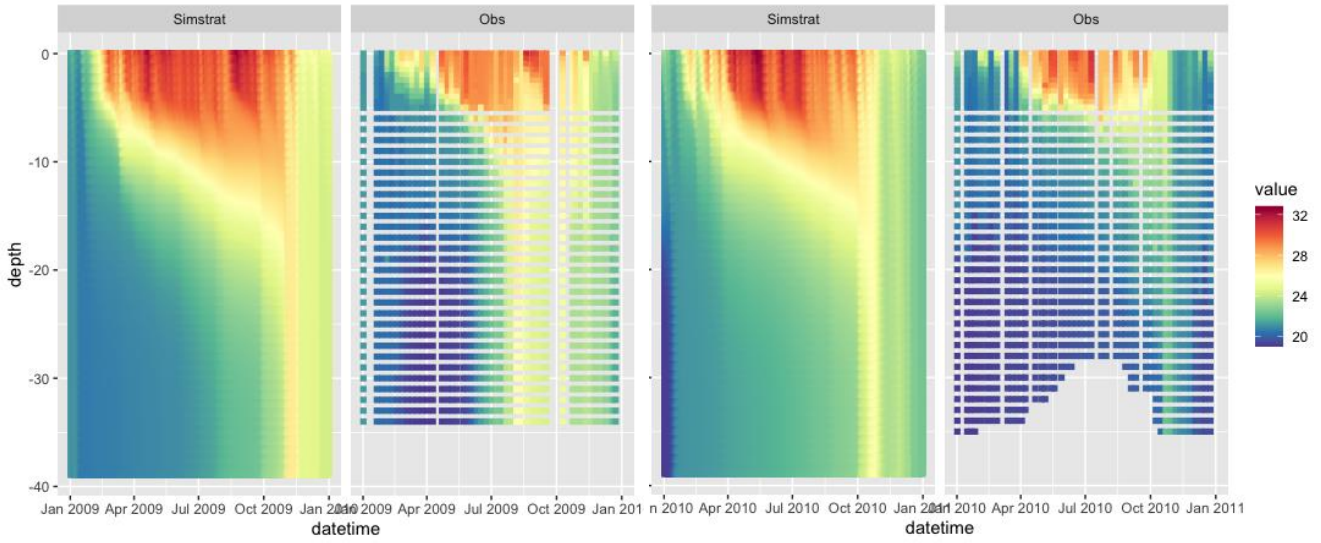

Figure B4 Simulated temperature profiles at Nam Theun 2, by Simstrat physical lake model without calibration of the a_{seiche} parameter and with an arbitrary k_d of 1.0 m^{-1}. Figures labeled "Simstrat" are simulated profiles and "obs" are the measured available thermal surveys.

APPENDIX C

Estimation of reservoir hypsography according to Imboden (1973)

Reservoir area at depth *z* is estimated from the following equations:

$$a_z = a_s(1 - z/z_{max})^q,$$

$$q = z_{max}/(z_{mean} - 1),$$

where a_z is area at depth z in m^2, a_s is the surface area in m^2, z_{max} is max depth in meters and z_{mean} is average depth in meters. In this study, a_s, z_{max} and z_{mean} were known characteristics, extracted from the GRanD database (Lehner et al. 2011).

APPENDIX D

Computation of energy budget components for the Bowen Ratio Energy Budget method

The Bowen Ratio Energy Budget (BREB) method is based on the conservation of energy law. It accounts for incoming, outgoing, and stored energy in a system. It can be expressed as follow (Lenters et al. 2005):

$$N = R_n + A_n + G_n - H - L,$$

where N is the change in heat storage of the water body, R_n is net radiation at the water surface, A_n is net advected energy, G_n is net energy exchange between the sediments and overlying water, H is sensible heat flux and L is latent heat flux. By rearranging the equation, evaporation (E, in mm day^{-1}) can be derived from latent heat (L) and water's latent heat of vaporisation (λ):

$$L = \lambda E,$$

$$E = \frac{R_n + A_n + G_n - H - N}{\lambda}$$

Latent heat if vaporisation is dependent of air temperature and is calculated as (McJannet et al. 2008):

$$\lambda = 2.501 - 2.361\mathrm{e}^{-3}\, T_a,$$

where T_a is air temperature in °C and λ is latent heat of vaporisation in MJ Kg^{-1}. Sensible heat flux is substituted by the Bowen ratio (Brutsaert 2013):

$$\beta = \frac{H}{L} = \frac{c_p \emptyset (T_s - T_a)}{\varepsilon_m \lambda (e_s^* - e_a)},$$

where c_p is specific heat of air at constant pressure (0.001013 MJ Kg^{-1}C^{-1}), $\emptyset$ is atmospheric pressure in kPa, T_s and T_a is temperature of the water surface and the air in °C, ε_m is the ratio of molecular weight of water to that of dry air (=0.622), e^*_s is saturation vapor pressure at water surface temperature and e_a is vapor pressure of the overlying air, both in kPa (McJannet et al. 2008; McMahon et al. 2013):

$$e_s^* = 0.6108 \exp\left(\frac{17.27T_s}{T_s+273.15}\right),$$

$$e_a = 0.6108 \exp\left(\frac{17.27T_{dew}}{T_{dew}+273.15}\right),$$

where T_{dew} is dew point temperature in °C. The ratio $c_p\emptyset/\varepsilon_m\lambda$ is also termed the psychrometric constant, γ. By combining equations, we obtain evaporation from the following equation, which constitutes the BREB method:

$$E = \frac{R_n+A_n+G_n-N}{\lambda(1+\beta)}.$$

The exchange of energy in a water body is usually governed by exchanges at the water surface and heat storage *in deep lakes* (stratified), rather than advected energy and sediment conduction (Henderson-sellers 1986). For *shallow lakes*, a sediment conduction can however be significant (Sturrock et al. 1992). Thus, the last equation can be furthered simplified to a reduced energy budget equation:

$$E = \frac{R_n+G_n-N}{\lambda(1+\beta)}.$$

Net radiation term (R_n) :

Net radiation (MJ m^{-2} day^{-1}) was calculated by combining net shortwave radiations (R_{ns}) with net longwave radiation (R_{nl}) at the water surface:

$$R_n = R_{ns} + R_{nl}.$$

Net shortwave radiations was obtained as a percent of measured incoming solar shortwave radiations (R_{is}) in relation with water surface albedo (α), which represents the radiations that are not reflected by the water surface:

$$R_{ns} = (1-\alpha)R_{is}.$$

Net longwave radiations was obtained by subtracting outgoing longwave radiation (R_{ol}) from measured incoming thermal longwave radiations (R_{il}):

$$R_{nl} = R_{il} - R_{ol}.$$

Outgoing longwave radiation was calculated from the Stefan-Boltzmann relationship:

$$R_{ol} = \varepsilon\sigma(T_s + 273.15)^4,$$

where σ is the Stefan-Boltzmann constant (4.903e^{-9} MJ m^{-2} K^{-1}), ε is emissivity of water (≈ 0.97) and T_s is water surface temperature in °C.

Heat storage term (N):

Changes in heat storage was calculated as follow:

$$N = \frac{\rho_w c_w}{a_s} \sum_z \left(\frac{\Delta T_z}{\Delta t} a_z \Delta_z\right),$$

where ρ_w is density of water (997.9 Kg m^{-3}), c_w is specific heat of water (0.00419 MJ Kg^{-1} °C^{-1}), a_s is the water body surface area in m^2, ΔT_z is change in mean lake temperature in °C at depth z over period Δt, a_z is lake area at depth z and Δ_z is discretized layer thickness in meters. Lake area at depth was estimated according to Imboden, 1973 (appendix C).

Sediment heat conduction term (G_n):

Sediment heat conduction might be significant in shallow water bodies, where there is high variability in bottom water temperature throughout the year. It was estimated as follow (Rogers et al. 1995):

$$G_n = K_{sed} \frac{dT}{dz},$$

where K_{sed} is the sediment heat transfer conductivity (1.2 W m^{-1} °C^{-1}) and dT/dz is the temperature gradient between the water and the sediments. This last term is estimated as follow:

$$\frac{dT}{dz} = \frac{T_{yr} - T_w}{Z_{sed}},$$

where T_{yr} is annual mean whole lake temperature, T_w is water temperature at the bottom of the water body and Z_{sed} is the distance over which sediment temperature would increase from T_{yr} to T_w in the relation was linear. Z_{sed} is assumed to be 2 meters in most situation, because temperature in sediments below that depth is generally constant over time (Ashton 1986).

APPENDIX E

List of used R libraries with corresponding authors

Library name	Citation
R software, R Studio	R Core Team (2021). R: A language and environment for statistical computing. R Foundation for Statistical Computing, Vienna, Austria.
kgc	Chelsey Bryant, Nicholas R. Wheeler, Franz Rubel and Roger H. French (2017). kgc: Koeppen-Geiger Climatic Zones. R package version 1.0.0.2.
LakeEnsemblR	Tadhg N. Moore, Jorrit P. Mesman, Robert Ladwig, Johannes Feldbauer, Freya Olsson, Rachel M. Pilla, Tom Shatwell, Jason J. Venkiteswaran, Austin D. Delany, Hilary Dugan, Kevin C. Rose, Jordan S. Read (in submission). LakeEnsemblR: An R package that facilitates ensemble modelling of lakes. Environ. Model. Softw.
lubridate	Garrett Grolemund, Hadley Wickham (2011). Dates and Times Made Easy with lubridate. Journal of Statistical Software, 40(3), 1-25.
ggmap	D. Kahle and H. Wickham. ggmap: Spatial Visualization with ggplot2. The R Journal, 5(1), 144-161.
ggnewscale	Elio Campitelli (2021). ggnewscale: Multiple Fill and Colour Scales in 'ggplot2'. R package version 0.4.5.
ggplot2	H. Wickham. ggplot2: Elegant Graphics for Data Analysis. Springer-Verlag New York, 2016.
ggpubr	Alboukadel Kassambara (2020). ggpubr: 'ggplot2' Based Publication Ready Plots. R package version 0.4.0.
mgcv	Wood, S.N. (2011) Fast stable restricted maximum likelihood and marginal likelihood estimation of semiparametric generalized linear models. Journal of the Royal Statistical Society (B) 73(1):3-36
tidyverse	Wickham et al., (2019). Welcome to the tidyverse. Journal of Open Source Software, 4(43), 1686.
TTR	Joshua Ulrich (2020). TTR: Technical Trading Rules. R package version 0.24.2.

APPENDIX F

Relationships and models between reservoir morphology and annual evaporation

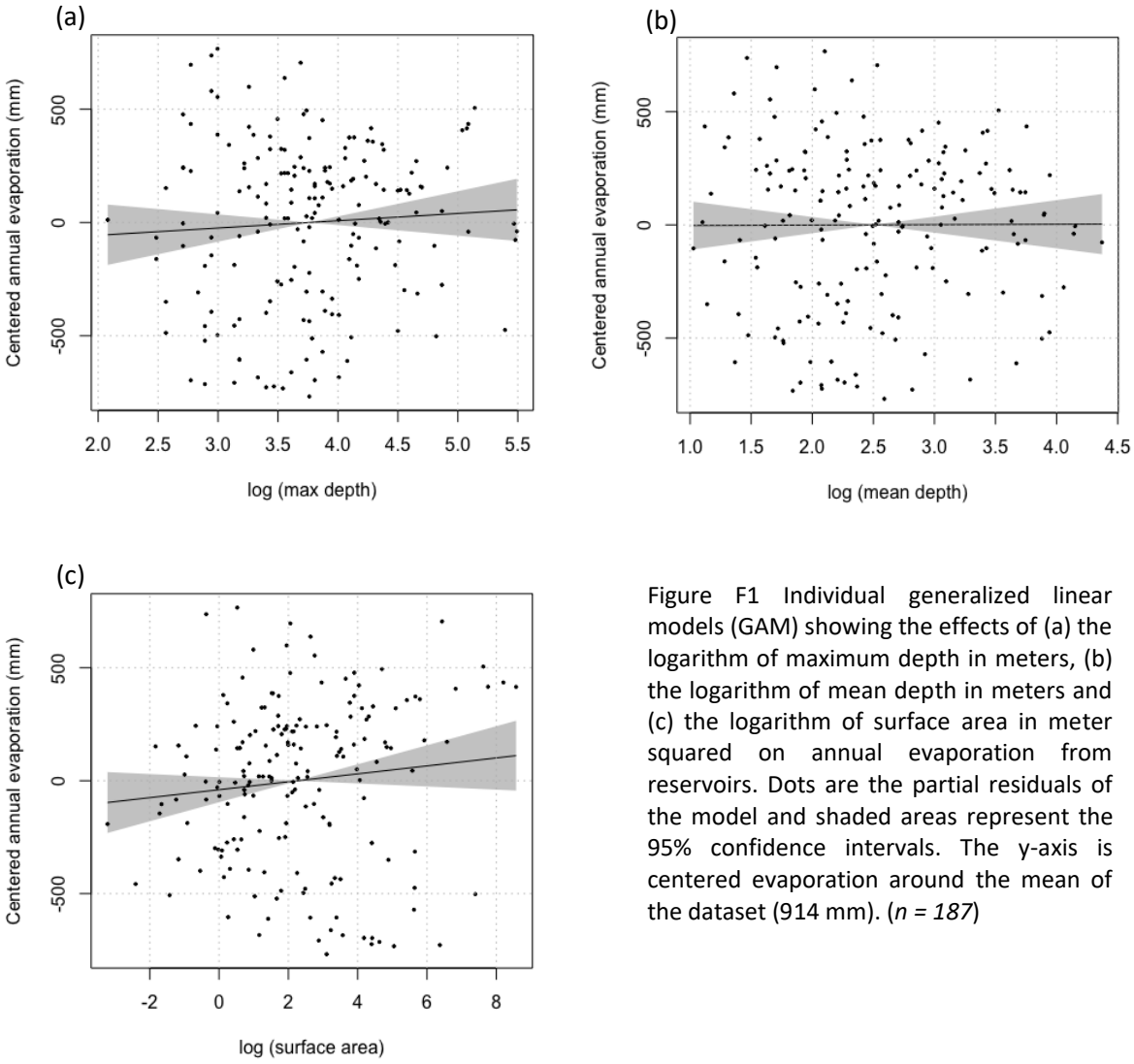

Figure F1 Individual generalized linear models (GAM) showing the effects of (a) the logarithm of maximum depth in meters, (b) the logarithm of mean depth in meters and (c) the logarithm of surface area in meter squared on annual evaporation from reservoirs. Dots are the partial residuals of the model and shaded areas represent the 95% confidence intervals. The y-axis is centered evaporation around the mean of the dataset (914 mm). (*n = 187*)

RÉFÉRENCES

Adams, E. E., Cosler, D. J., & Helfrich, K. R. (1990). Evaporation from heated water bodies: predicting combined forced plus free convection. *Water Resources Research*, *26*(3), 425-435.

Arp, C. D., Jones, B. M., & Grosse, G. (2013). Recent lake ice-out phenology within and among lake districts of Alaska, USA. *Limnology and Oceanography*, *58*(6), 2013-2028.

Assouline, S., & Mahrer, Y. (1993). Evaporation from Lake Kinneret: 1. Eddy correlation system measurements and energy budget estimates. *Water Resources Research*, *29*(4), 901-910.

Beven, K. (2006). A manifesto for the equifinality thesis. *Journal of hydrology*, *320*(1-2), 18-36.

Blanken, P. D., Spence, C., Hedstrom, N., & Lenters, J. D. (2011). Evaporation from Lake Superior: 1. Physical controls and processes. *Journal of Great Lakes Research*, *37*(4), 707-716.

Boehrer, B., & Schultze, M. (2009). Density stratification and stability. *Biogeochemistry of inland waters*, 625-635.

Bowen, I. S. (1926). The ratio of heat losses by conduction and by evaporation from any water surface. *Physical review*, *27*(6), 779.

Brutsaert, W. (2013). *Evaporation into the atmosphere: theory, history and applications* (Vol. 1). Springer Science & Business Media.

Brutsaert, W., & Parlange, M. B. (1998). Hydrologic cycle explains the evaporation paradox. *Nature*, *396*(6706), 30-30.

Burba, G., & Anderson, D. (2010). *A brief practical guide to eddy covariance flux measurements: principles and workflow examples for scientific and industrial applications*. Li-Cor Biosciences.

Chanudet, V., Guédant, P., Rode, W., Godon, A., Guérin, F., Serça, D., ... & Descloux, S. (2016). Evolution of the physico-chemical water quality in the Nam Theun 2 Reservoir and downstream rivers for the first 5 years after impoundment. *Hydroécologie Appliquée*, *19*, 27-61.

Choudhury, B. J. (1997). Global pattern of potential evaporation calculated from the Penman-Monteith equation using satellite and assimilated data. *Remote Sensing of Environment*, *61*(1), 64-81.

Clement, R. (1999). EdiRe data software. *Edinburgh, Scotland: The University of Edinburgh*, available online: http://www.geos. ed.ac.uk/abs/research/micromet/EdiRe/

Cogley, J. G. (1979). The albedo of water as a function of latitude. *Monthly Weather Review*, *107*(6), 775-781.

Condie, S. A., & Webster, I. T. (1997). The influence of wind stress, temperature, and humidity gradients on evaporation from reservoirs. *Water Resources Research*, *33*(12), 2813-2822.

Copernicus Climate Change Service (2017): ERA5: Fifth generation of ECMWF atmospheric reanalyses of the global climate, Coperni- cus Climate Change Service Climate Data Store (CDS), available at: https://cds.climate.copernicus.eu/cdsapp#!/home.

Craig, I., Schmidt, E., Green, A., & Scobie, M. (2005). Controlling evaporation from on-farm storages. In *Irrigation Australia 2005: Irrigation Association of Australia National Conference and Exhibition: Proceedings*. Irrigation Australia Ltd.

Dake, J. M. (1972). Evaporative cooling of a body of water. *Water Resources Research*, *8*(4), 1087-1091.

Dalton, J. (1802). Experimental essays on the constitution of mixed gases. *Manchester Literary and Philosophical Society Memo*, *5*, 535-602.

Dawson, C. W., Abrahart, R. J., & See, L. M. (2007). HydroTest: a web-based toolbox of evaluation metrics for the standardised assessment of hydrological forecasts. *Environmental M*

Descloux, S., Guedant, P., Phommachanh, D., & Luthi, R. (2016). Main features of the Nam Theun 2 hydroelectric project (Lao PDR) and the associated environmental monitoring programmes. *Hydroécologie Appliquée*, *19*, 5-25.

Deshmukh, C., Serça, D., Delon, C., Tardif, R., Demarty, M., Jarnot, C., ... & Guérin, F. (2014). Physical controls on CH 4 emissions from a newly flooded subtropical freshwater hydroelectric reservoir: Nam Theun 2. *Biogeosciences*, *11*(15), 4251-4269.

Diks, C. G., & Vrugt, J. A. (2010). Comparison of point forecast accuracy of model averaging methods in hydrologic applications. *Stochastic Environmental Research and Risk Assessment*, *24*(6), 809-820.

Dingman, S. L. (2015). *Physical hydrology*. Waveland press.

Dörnhöfer, K., & Oppelt, N. (2016). Remote sensing for lake research and monitoring–Recent advances. *Ecological Indicators*, *64*, 105-122.

Du, Q., Liu, H. Z., Liu, Y., Wang, L., Xu, L. J., Sun, J. H., & Xu, A. L. (2018). Factors controlling evaporation and the CO2 flux over an open water lake in southwest of China on multiple temporal scales. *International Journal of Climatology*, *38*(13), 4723-4739.

Duan, Q., Ajami, N. K., Gao, X., & Sorooshian, S. (2007). Multi-model ensemble hydrologic prediction using Bayesian model averaging. *Advances in water Resources*, *30*(5), 1371-1386.

Fiedler, P. C. (2010). Comparison of objective descriptions of the thermocline. *Limnology and Oceanography: Methods*, *8*(6), 313-325.

Finch, J., & Calver, A. (2008). Methods for the quantification of evaporation from lakes (prepared for the World Meteorological Organization's Commission for Hydrology).

Fogarty, M. C., Fewings, M. R., Paget, A. C., & Dierssen, H. M. (2018). The influence of a sandy substrate, seagrass, or highly turbid water on albedo and surface heat flux. *Journal of Geophysical Research: Oceans*, *123*(1), 53-73.

Fournier, J., Thiboult, A., Nadeau, D. F., Vercauteren, N., Anctil, F., Parent, A. C., ... & Tremblay, A. (2021). Evaporation from boreal reservoirs: A comparison between eddy covariance observations and estimates relying on limited data. *Hydrological Processes*, *35*(8), e14335.

Friedrich, K., Grossman, R. L., Huntington, J., Blanken, P. D., Lenters, J., Holman, K. D., ... & Kowalski, T. (2018). Reservoir evaporation in the Western United States: current science, challenges, and future needs. *Bulletin of the American Meteorological Society*, *99*(1), 167-187.

Fritsch, J. M., Hilliker, J., Ross, J., & Vislocky, R. L. (2000). Model consensus. *Weather and forecasting*, *15*(5), 571-582.

Gan, G., & Liu, Y. (2020). Heat storage effect on evaporation estimates of China's largest freshwater lake. *Journal of Geophysical Research: Atmospheres*, *125*(19), e2019JD032334.

Gaudard, A., Råman Vinnå, L., Bärenbold, F., Schmid, M., & Bouffard, D. (2019). Toward an open access to high-frequency lake modeling and statistics data for scientists and practitioners–the case of Swiss lakes using Simstrat v2. 1. *Geoscientific Model Development*, *12*(9), 3955-3974.

Gaudard, A., Schwefel, R., Vinnå, L. R., Schmid, M., Wüest, A., & Bouffard, D. (2017). Optimizing the parameterization of deep mixing and internal seiches in one-dimensional hydrodynamic models: a case study with Simstrat v1. 3. *Geoscientific Model Development*, *10*(9), 3411-3423.

Giardino, C., Bresciani, M., Cazzaniga, I., Schenk, K., Rieger, P., Braga, F., ... & Brando, V. E. (2014a). Evaluation of multi-resolution satellite sensors for assessing water quality and bottom depth of Lake Garda. *Sensors*, *14*(12), 24116-24131.

Giardino, C., Bresciani, M., Stroppiana, D., Oggioni, A., & Morabito, G. (2014b). Optical remote sensing of lakes: an overview on Lake Maggiore. *Journal of Limnology*, *73*.

Gorham, E., & Boyce, F. M. (1989). Influence of lake surface area and depth upon thermal stratification and the depth of the summer thermocline. *Journal of Great Lakes Research*, *15*(2), 233-245.

Goudsmit, G. H., Burchard, H., Peeters, F., & Wüest, A. (2002). Application of k-ϵ turbulence models to enclosed basins: The role of internal seiches. *Journal of Geophysical Research: Oceans*, *107*(C12), 23-1.

Henderson-Sellers, B. (1986). Calculating the surface energy balance for lake and reservoir modeling: A review. *Reviews of Geophysics*, *24*(3), 625-649.

Hersbach, H., Bell, B., Berrisford, P., Hirahara, S., Horányi, A., Muñoz-Sabater, J., ... & Thépaut, J. N. (2020). The ERA5 global reanalysis. *Quarterly Journal of the Royal Meteorological Society*, *146*(730), 1999-2049.

Hoekstra, A. Y., & Mekonnen, M. M. (2011). Global water scarcity: the monthly blue water footprint compared to blue water availability for the world's major basins.

Hondzo, M., & Stefan, H. G. (1993). Lake water temperature simulation model. Journal of Hydraulic Engineering, 119(11), 1251-1273.

Houser, J. N. (2006). Water color affects the stratification, surface temperature, heat content, and mean epilimnetic irradiance of small lakes. *Canadian Journal of Fisheries and Aquatic Sciences*, *63*(11), 2447-2455.

Huntington, T. G. (2006). Evidence for intensification of the global water cycle: Review and synthesis. *Journal of Hydrology*, *319*(1-4), 83-95

Huokuna, M., Morris, M., Beltaos, S., & Burrell, B. C. (2022). Ice in reservoirs and regulated rivers. *International Journal of River Basin Management*, *20*(1), 1-16.

Imboden, D. M. (1973). Limnologische Transport-und Nährstoffmodelle. *Schweizerische Zeitschrift für Hydrologie*, *35*(1), 29-68.

Irmak, S., Skaggs, K. E., & Chatterjee, S. (2014). A review of the Bowen ratio surface energy balance method for quantifying evapotranspiration and other energy fluxes. *Transactions of the ASABE*, *57*(6), 1657- 1674.

Jung, M., Reichstein, M., Ciais, P., Seneviratne, S. I., Sheffield, J., Goulden, M. L., ... & Zhang, K. (2010). Recent decline in the global land evapotranspiration trend due to limited moisture supply. *Nature*, *467*(7318), 951-954.

Kirk, J. T. (1985). Effects of suspensoids (turbidity) on penetration of solar radiation in aquatic ecosystems. *Hydrobiologia*, *125*(1), 195-208.

Kirk, J. T. (1994). *Light and photosynthesis in aquatic ecosystems*. Cambridge university press.

Kling, G. W. (1988). Comparative transparency, depth of mixing, and stability of stratification in lakes of Cameroon, West Africa 1. *Limnology and Oceanography*, *33*(1), 27-40.

Koutsoyiannis, D. (2020). Revisiting the global hydrological cycle: is it intensifying? *Hydrology and Earth System Sciences*, *24*(8), 3899-3932.

Kurc, S. A., & Small, E. E. (2004). Dynamics of evapotranspiration in semiarid grassland and shrubland ecosystems during the summer monsoon season, central New Mexico. *Water Resources Research*, *40*(9).

Lehner, B., C. Reidy Liermann, C. Revenga, C. Vörösmarty, B. Fekete, P. Crouzet, P. Döll, M. Endejan, K. Frenken, J. Magome, C. Nilsson, J.C. Robertson, R. Rodel, N. Sindorf, and D. Wisser. (2011). High- resolution mapping of the world's reservoirs and dams for sustainable river-flow management. Frontiers in Ecology and the Environment 9 (9): 494-502.

Lenters, J. D., Kratz, T. K., & Bowser, C. J. (2005). Effects of climate variability on lake evaporation: Results from a long-term energy budget study of Sparkling Lake, northern Wisconsin (USA). *Journal of Hydrology*, *308*(1-4), 168-195.

Leppäranta, M. (2010). Modelling the formation and decay of lake ice. In *The impact of climate change on European lakes* (pp. 63-83). Springer, Dordrecht.

Leppäranta, M. (2014). *Freezing of lakes and the evolution of their ice cover*. Springer Science & Business Media.

Lewis Jr, W. M. (1996). Tropical lakes: how latitude makes a difference. *Perspectives in tropical limnology*, *4364*, 43-64.

Majidi, M., Alizadeh, A., Farid, A., & Vazifedoust, M. (2015). Estimating evaporation from lakes and reservoirs under limited data co

McJannet, D. L., Webster, I. T., Stenson, M. P., & Sherman, B. S. (2008). *Estimating open water evaporation for the Murray-darling basin: a report to the Australian government from the CSIRO Murray-Darling basin sustainable yields project* (Vol. 50). Melbourne: CSIRO.

McJannet, D. L., Webster, I. T., & Cook, F. J. (2012). An area-dependent wind function for estimating open water evaporation using land-based meteorological data. *Environmental modelling & software*, *31*, 76-83.

McMahon, T. A., Peel, M. C., Lowe, L., Srikanthan, R., & McVicar, T. R. (2013). Estimating actual, potential, reference crop and pan evaporation using standard meteorological data: a pragmatic synthesis. *Hydrology and Earth System Sciences*, *17*(4), 1331-1363.

McVicar, T. R., Roderick, M. L., Donohue, R. J., Li, L. T., Van Niel, T. G., Thomas, A., ... & Dinpashoh, Y. (2012). Global review and synthesis of trends in observed terrestrial near-surface wind speeds: Implications for evaporation. *Journal of Hydrology*, *416*, 182-205.

Mekonnen, M. M., & Hoekstra, A. Y. (2016). Four billion people facing severe water scarcity. *Science advances*, *2*(2), e1500323.

Meng, X., Liu, H., Du, Q., Xu, L., & Liu, Y. (2020). Evaluation of the performance of different methods for estimating evaporation over a highland open freshwater lake in mountainous area. *Water*, *12*(12), 3491.

Miralles, D. G., Holmes, T. R. H., De Jeu, R. A. M., Gash, J. H., Meesters, A. G. C. A., & Dolman, A. J. (2011). Global land-surface evaporation estimated from satellite-based observations. *Hydrology and Earth System Sciences*, *15*(2), 453-469.

Moore, T. N., Mesman, J. P., Ladwig, R., Feldbauer, J., Olsson, F., Pilla, R. M., ... & Read, J. S. (2021). LakeEnsemblR: An R package that facilitates ensemble modelling of lakes. *Environmental Modelling & Software*, 105101.

Monismith, S. G., & MacIntyre, S. (2009). The surface mixed layer in lakes and reservoirs. *Biogeochemistry of inland waters*, 636-650.

Morton, F. I. "Evaporation research—a critical review and its lessons for the environmental sciences." *Critical reviews in environmental science and technology* 24.3 (1994): 237-280.

Muñoz Sabater, J., (2019): ERA5-Land hourly data from 1981 to present. Copernicus Climate Change Service (C3S) Climate Data Store (CDS).

Nordbo, A., Launiainen, S., Mammarella, I., Leppäranta, M., Huotari, J., Ojala, A., & Vesala, T. (2011). Long-term energy flux measurements and energy balance over a small boreal lake using eddy covariance technique. *Journal of Geophysical Research: Atmospheres*, *116*(D2).

Oke, T. R. (1987). Boundary layer climates, 2nd (ed.) Routledge. *London and Wiley, New York*.

Oki, T., & Kanae, S. (2006). Global hydrological cycles and world water resources. *science*, *313*(5790), 1068-1072.

R Core Team (2021). R: A language and environment for statistical computing. R Foundation for Statistical Computing, Vienna, Austria. URL https://www.R-project.org/.

Reichstein, M., Falge, E., Baldocchi, D., Papale, D., Aubinet, M., Berbigier, P., ... & Valentini, R. (2005). On the separation of net ecosystem exchange into assimilation and ecosystem respiration: review and improved algorithm. *Global change biology*, *11*(9), 1424-1439.

Ritchie, H., & Roser, M. (2017). *Water use and stress.* Our World in Data. https://ourworldindata.org/water-use-stress

Roderick, M. L., & Farquhar, G. D. (2002). The cause of decreased pan evaporation over the past 50 years. *science*, *298*(5597), 1410-1411.

Rosenberry, D. O., Winter, T. C., Buso, D. C., & Likens, G. E. (2007). Comparison of 15 evaporation methods applied to a small mountain lake in the northeastern USA. *Journal of hydrology*, *340*(3-4), 149-166.

Rust, F., Bodmer, P., & Del Giorgio, P. (2022). Modeling the spatial and temporal variability in surface water CO2 and CH4 concentrations in a newly created complex of boreal hydroelectric reservoirs. *Science of The Total Environment*, *815*, 152459.

Ryan, P. J., Harleman, D. R., & Stolzenbach, K. D. (1974). Surface heat loss from cooling ponds. *Water resources research*, *10*(5), 930-938.

Sacks, L. A., Lee, T. M., & Radell, M. J. (1994). Comparison of energy-budget evaporation losses from two morphometrically different Florida seepage lakes. *Journal of Hydrology*, *156*(1-4), 311-334.

Saloranta, T. M., & Andersen, T. (2007). MyLake—A multi-year lake simulation model code suitable for uncertainty and sensitivity analysis simulations. *Ecological modelling*, *207*(1), 45-60.

Savage, M. J., Everson, C. S., & Metelerkamp, B. R. (2009). Bowen ratio evaporation measurement in a remote montane grassland: Data integrity and fluxes. *Journal of Hydrology*, *376*(1-2), 249-260.

Schmid, M., & Köster, O. (2016). Excess warming of a central european lake driven by solar brightening. *Water Resources Research*, *52*(10), 8103-8116.

Schneider, P., & Hook, S. J. (2010). Space observations of inland water bodies show rapid surface warming since 1985. *Geophysical Research Letters*, *37*(22).

Seidel, S. D., & Yang, D. (2020). The lightness of water vapor helps to stabilize tropical climate, Sci. Adv., 6, eaba1951.

Sene, K. J., Gash, J. H. C., & McNeil, D. D. (1991). Evaporation from a tropical lake: comparison of theory with direct measurements. *Journal of Hydrology*, *127*(1-4), 193-217.

Siemens, K., Dibike, Y., Shrestha, R. R., & Prowse, T. (2021). Runoff projection from an alpine watershed in western Canada: application of a snowmelt runoff model. *Water*, *13*(9), 1199.

Singh, V. P., & Xu, C. Y. (1997). Evaluation and generalization of 13 mass-transfer equations for determining free water evaporation. *Hydrological Processes*, *11*(3), 311-323.

Singh, V. P., & Xu, C. Y. (1997). Sensitivity of mass transfer-based evaporation equations to errors in daily and monthly input data. *Hydrological processes*, *11*(11), 1465-1473.

Spigel, R. H., & Imberger, J. (1980). The classification of mixed-layer dynamics of lakes of small to medium size. *Journal of physical oceanography*, *10*(7), 1104-1121.

Sturrock, A. M., Winter, T. C., & Rosenberry, D. O. (1992). Energy budget evaporation from Williams Lake: A closed lake in north central Minnesota. *Water Resources Research*, *28*(6), 1605-1617.

Subin, Z. M., Riley, W. J., & Mironov, D. (2012). An improved lake model for climate simulations: Model structure, evaluation, and sensitivity analyses in CESM1. *Journal of Advances in Modeling Earth Systems*, *4*(1).

Trenberth, K. E., Fasullo, J. T., & Kiehl, J. (2009). Earth's global energy budget. *Bulletin of the American Meteorological Society*, *90*(3), 311-324.

Wang, K., & Dickinson, R. E. (2012). A review of global terrestrial evapotranspiration: Observation, modeling, climatology, and climatic variability. *Reviews of Geophysics*, *50*(2).

Wang, W., Lee, X., Xiao, W., Liu, S., Schultz, N., Wang, Y., ... & Zhao, L. (2018). Global lake evaporation accelerated by changes in surface energy allocation in a warmer climate. *Nature Geoscience*, *11*(6), 410-414.

Wang, W., Xiao, W., Cao, C., Gao, Z., Hu, Z., Liu, S., ... & Lee, X. (2014). Temporal and spatial variations in radiation and energy balance across a large freshwater lake in China. *Journal of Hydrology*, *511*, 811-824.

Winter, T. C., Rosenberry, D. O., & Sturrock, A. M. (1995). Evaluation of 11 equations for determining evaporation for a small lake in the north central United States. *Water Resources Research*, *31*(4), 983-993.

Woolway, R. I., Kraemer, B. M., Lenters, J. D., Merchant, C. J., O'Reilly, C. M., & Sharma, S. (2020). Global lake responses to climate change. *Nature Reviews Earth & Environment*, *1*(8), 388-403.

Wu, P., Christidis, N., & Stott, P. (2013). Anthropogenic impact on Earth's hydrological cycle. *Nature Climate Change*, *3*(9), 807-810.

Wüest, A., & Lorke, A. (2003). Small-scale hydrodynamics in lakes. *Annual Review of fluid mechanics*, *35*(1), 373-412.

Wurbs, R. A., & Ayala, R. A. (2014). Reservoir evaporation in Texas, USA. *Journal of Hydrology*, *510*, 1-9.

Zhao, G., & Gao, H. (2019). Estimating reservoir evaporation losses for the United States: Fusing remote sensing and modeling approaches. *Remote Sensing of Environment*, *226*, 109-124.